2
M1.X
GCA-TR-72-1-N

MARCH 7, 1970 SOLAR ECLIPSE INVESTIGATION

Carl A. Accardo

(NASA-CR-130698) MARCH 7, 1970 SOLAR ECLIPSE INVESTIGATION Final Report (GCA Corp.) 81 p HC $6.25 CSCL 03C

N73-17843

Unclas

G3/30 16789

GCA CORPORATION

Bedford, Massachusetts

FINAL REPORT

Contract No. NASW-1993

Prepared for

NATIONAL AERONAUTICS AND SPACE ADMINISTRATION
HEADQUARTERS
WASHINGTON, D. C.

October 1972

71

GCA-TR-72-1-N

MARCH 7, 1970 SOLAR ECLIPSE INVESTIGATION

Carl A. Accardo

GCA CORPORATION
GCA TECHNOLOGY DIVISION
Bedford, Massachusetts

FINAL REPORT

Contract No. NASW-1993

October 1972

Prepared for

NATIONAL AERONAUTICS AND SPACE ADMINISTRATION
HEADQUARTERS
WASHINGTON, D.C.

TABLE OF CONTENTS

MARCH 7, 1970 SOLAR ECLIPSE INVESTIGATION

by
Carl A. Accardo
GCA Corporation, GCA Technology Division, Bedford, Massachusetts

SECTION I

INTRODUCTION

The program described represents a continuation of studies from rockets directed toward establishing the solar X-ray fluxes during the 7 March 1970 total eclipse over the North American continent. A map of the eclipse path prepared by Dr. L. G. Smith is illustrated in Figure 1. The measured absorption profiles for the residual X-rays are useful in establishing their contribution to the D and E region ionization during the eclipse. The studies were performed with two Nike-Apache payloads launched over Wallops Island, Virginia. In addition to three X-ray detectors in the 1 to 8Å, 8 to 20Å and 44 to 60Å bands, there was included in the payloads two additional experiments for which GCA was delegated the additional responsibility of integrating into the payloads. These were an electric field experiment and an epithermal photoelectron experiment. The latter two packages were provided by participating scientists at the Goddard Space Flight Center and Lockheed Aircraft Corporation, respectively. The electric field experiment also contained a propagation experiment in which an on-board receiver tuned at 17.8 Mc detects a ground-based radio transmission to establish electron density profiles.

In addition to the two payloads designed and fabricated under Contract No. NASW-1993, 44 to 60Å counters were carried in four other GCA-University of Illinois Nike Apache payloads fabricated under the NASW-1994 program. The report describes the X-ray instrumentation, payload description, flight circumstances and finally, the X-ray results obtained. The various computer codes employed for the purpose of reducing the telemetered data as well as the eclipse codes are included in the report.

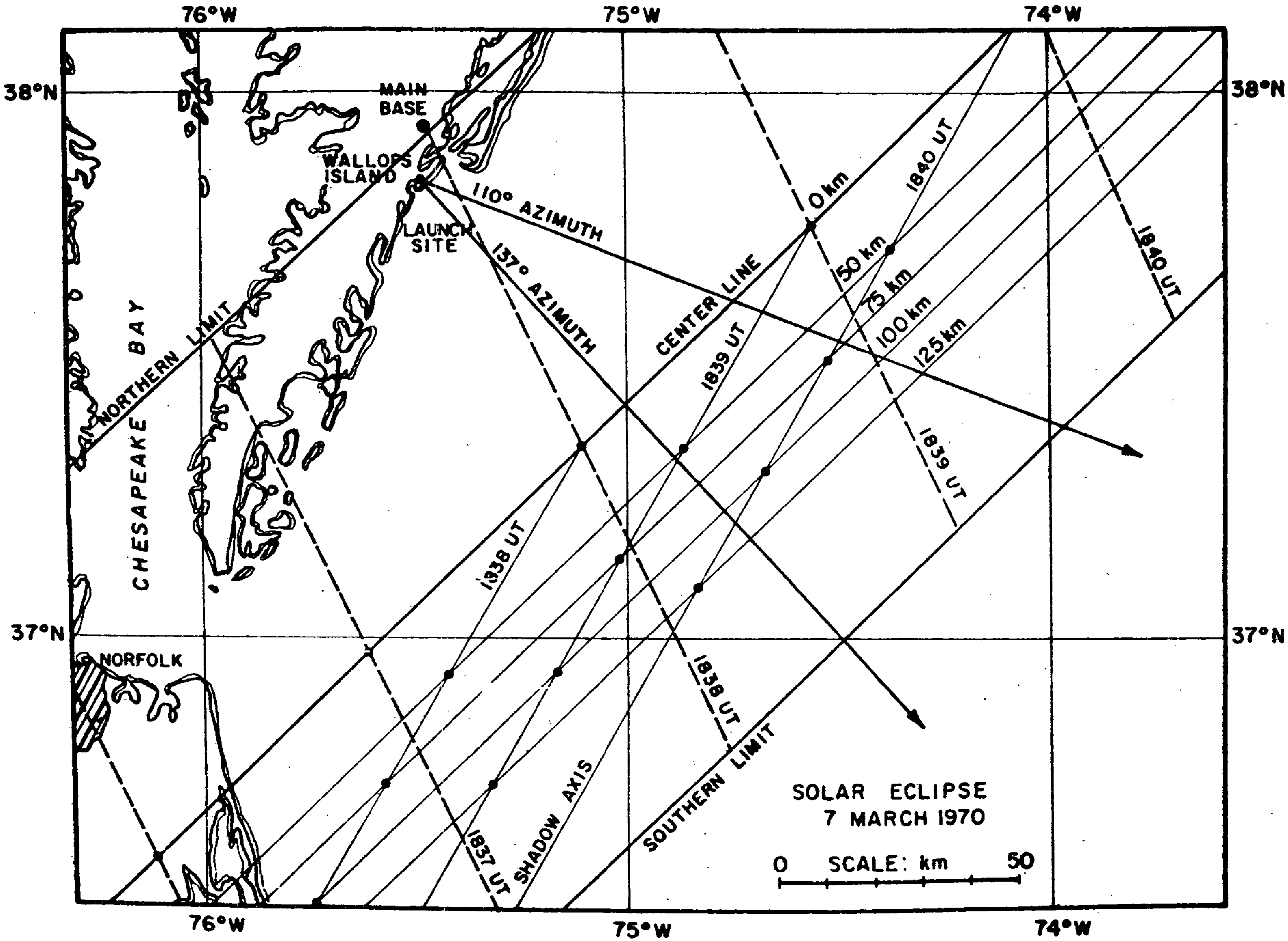

Figure 1. March 1970 solar eclipse path over Wallops Island, Va.

SECTION II

DETECTOR DESCRIPTION

The X-ray Geiger counters were fabricated by Tracerlab Corp., Waltham, Massachusetts to specifications requested by the experimenter. The counters were cylindrical and possessed an overall length of approximately 3 inches with a 1 inch diameter. The counter gas fill consisted of a mixture of neon/isobutane at one-half atmospheric pressure. The isobutane serves to quench the discharge after each ionizing pulse. X-rays are admitted to the counter through an appropriate aperture located within the cylindrical section.

The response of the counters is given by the simple relationship

$$e_{ff} = e^{\left[-\frac{\mu}{p}\rho x\right]_{\text{window}}}\left(1-e^{\left[-\frac{\mu}{p}\rho x\right]_{\text{gas}}}\right)$$

Here the counter efficiency is simply the product of the X-ray transmission through the window material and their subsequent absorption in the gas fill. The particular response of the counters is obtained by the proper selection of window material and gas fill. For the bands 44 to 60Å, 8 to 20Å and 1 to 8Å, this is achieved by means of mylar, aluminum and beryllium windows, respectively. The response for each of the counters is shown in Figures 2, 3, and 4.

The counters were located in the payload on a single deck as may be seen in Figure 5. In order to protect the detectors during launch and powered flight, a protective door was installed in the skin of the payload and ejected at approximately 60 km during ascent.

Signal processing of the Geiger counter outputs was accomplished by means of the circuitry illustrated in the Figure 6 block diagram. The Geiger pulses are amplified and shaped, providing a pulse of fixed amplitude and duration. A staircase generator was used as a digital to analog converter. The type of signal output resulting from this circuit is discussed in somewhat more detail in the reprint of scientific results obtained included in the Appendix.

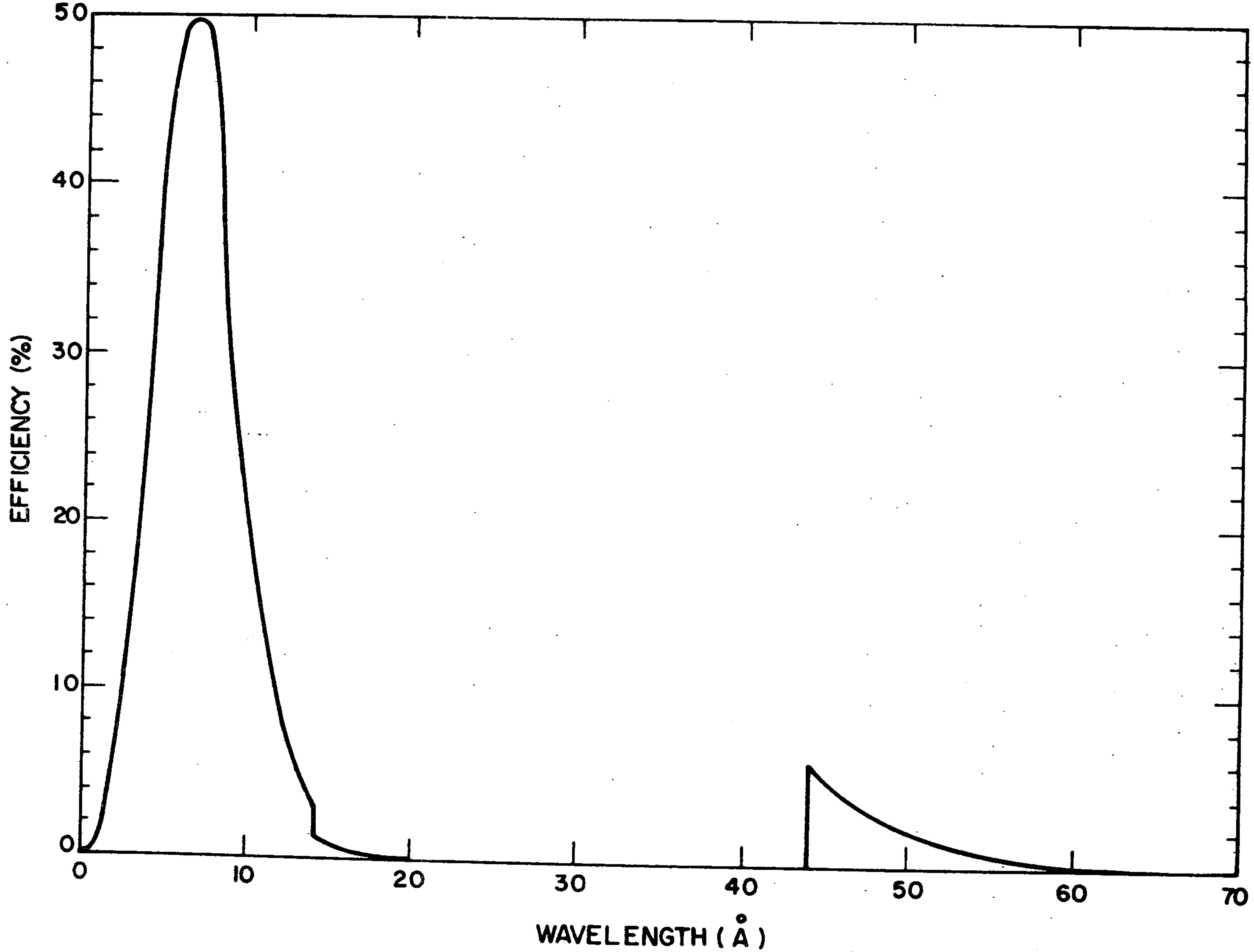

Figure 2. 44-60Å counter efficiency; 1/4 Mil Mylar; 1.27 cm-atm Neon.

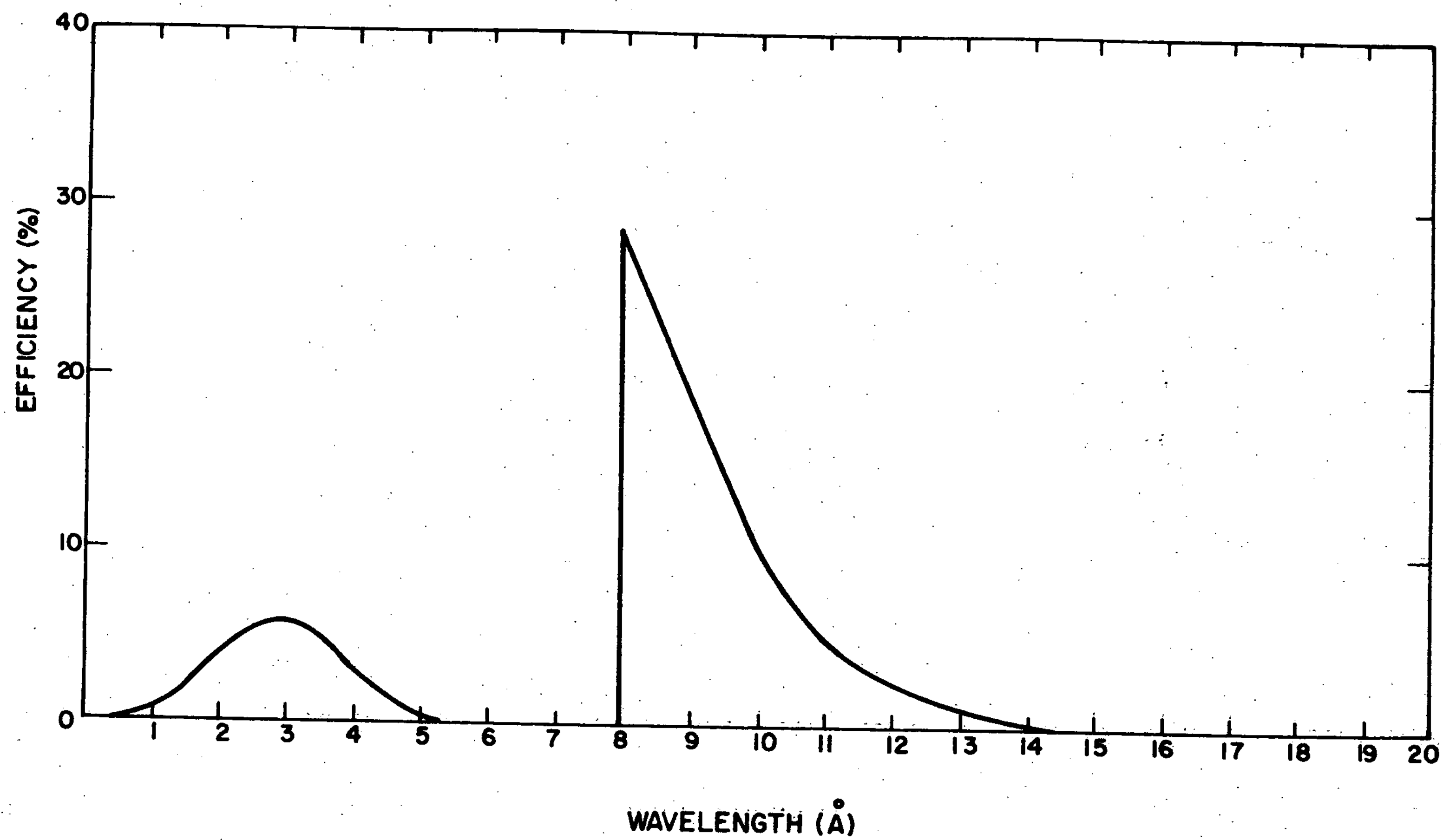

Figure 3. 8-20Å counter efficiency; 0.5 Mil Aluminum; 1.27 cm-atm Neon.

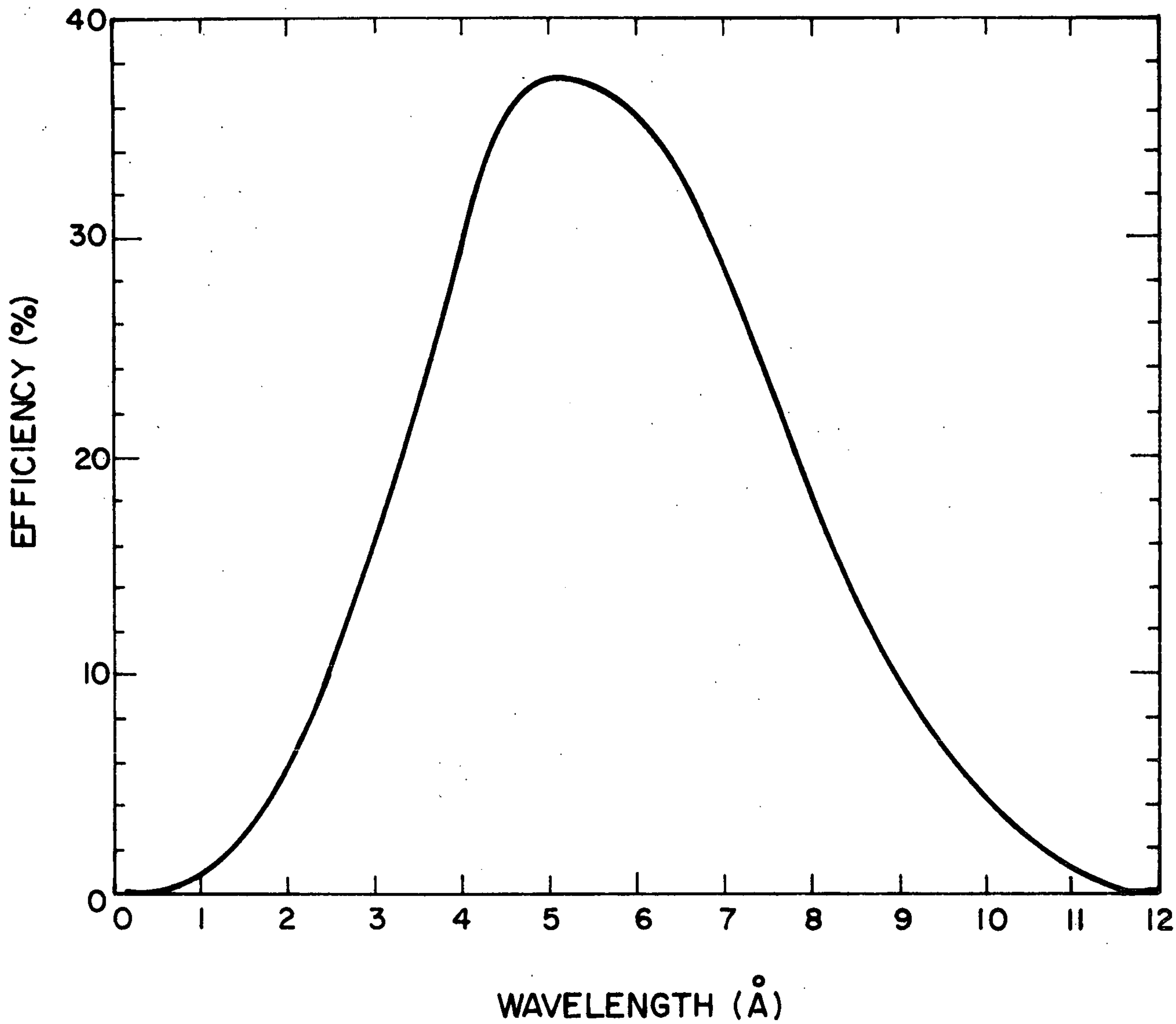

Figure 4. 2-10Å counter efficiency; 2 mil Be, 1.27 cm-atm Neon.

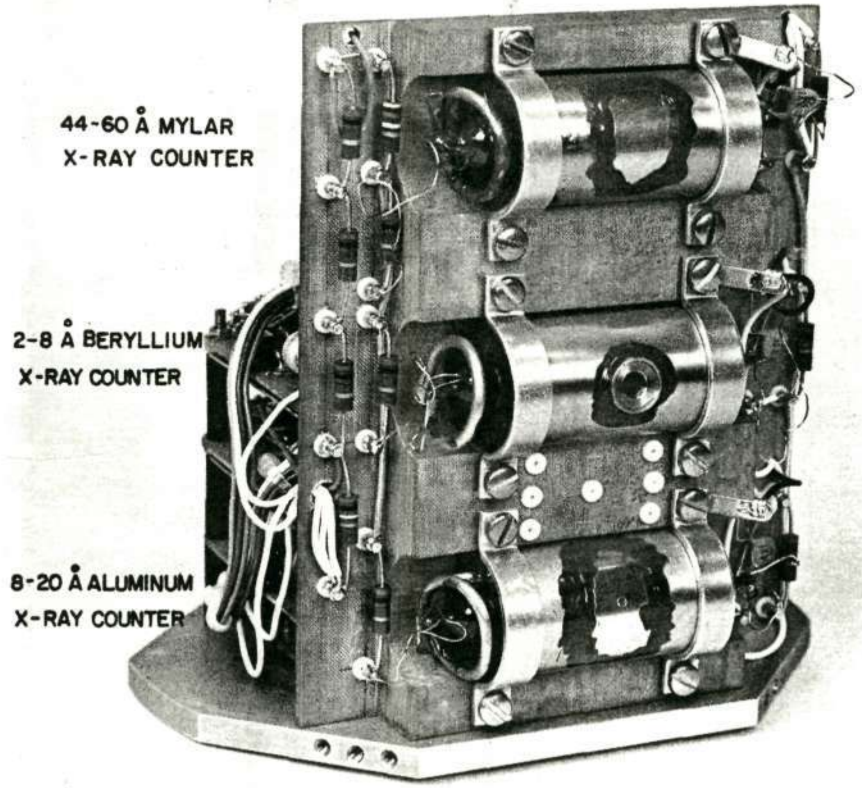

Figure 5. X-ray Geiger counter deck.

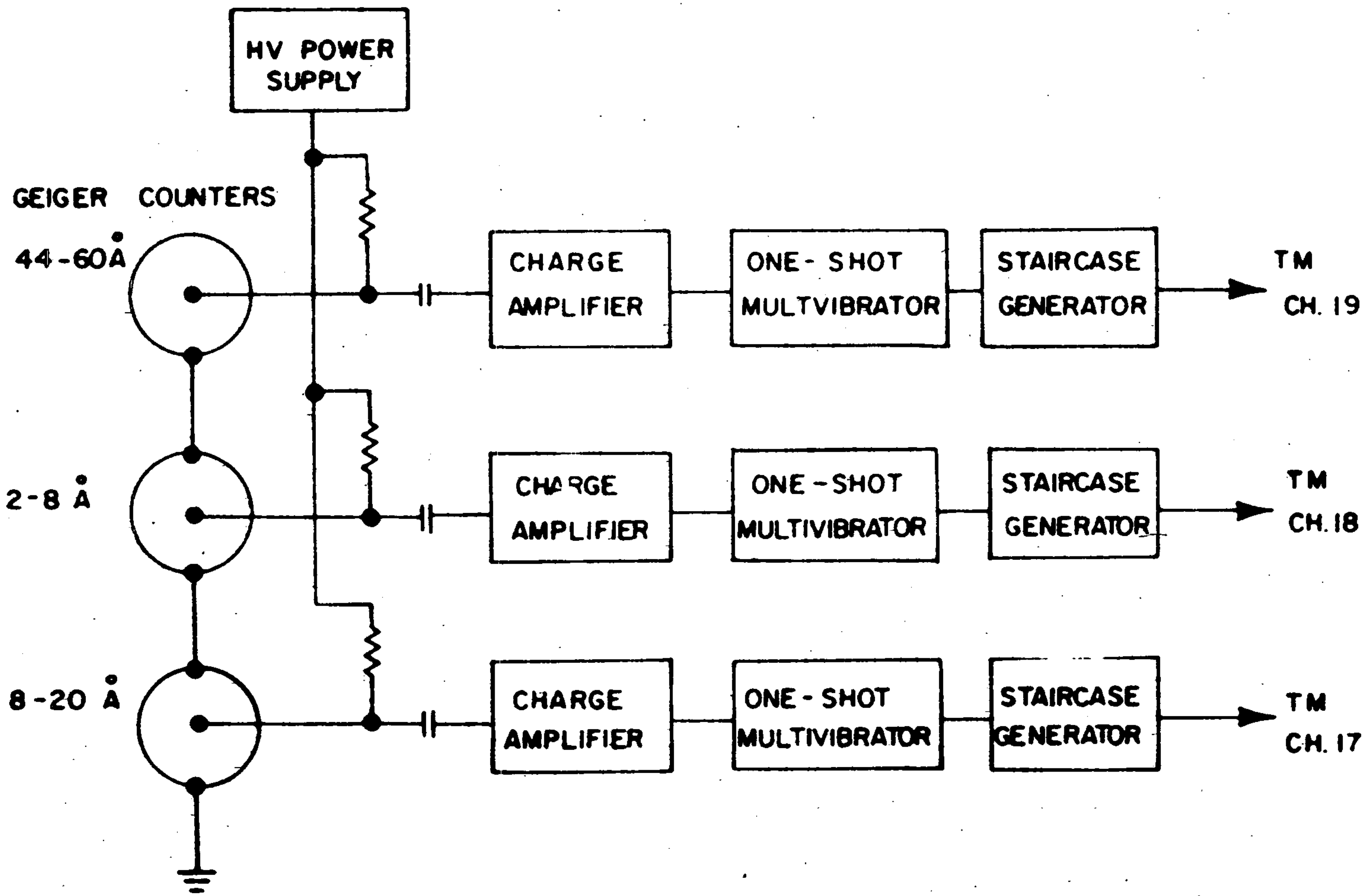

Figure 6. Block diagram - rocket solar X-ray experiment.

SECTION III

PAYLOAD DESCRIPTION

The payloads were designed using standard NASA Nike-Apache hardware consisting of a spun 11° aluminum nose cone and a 6 5/8"dia. aluminum shell and deck structure. For the purpose of determining vehicle roll altitude a solar aspect sensor and two magnetometers were included. As mentioned earlier, experiments provided by NASA and Lockheed Corporation were also integrated into both payloads. The NASA electric-field experiment required deployment of a symmetric pair of antennas, each extending radially outward 20 feet through openings in the payload skin. These antennas were of the unfurlable type and were deployed at a rate of 0.33 feet/sec beginning at 90 km.

The Lockheed electron analyzer experiment consisted of a single deck. Exposure of the sensor to the ambient was accomplished after ejection of the protective door which simultaneously exposed the solar aspect sensor and Geiger counters.

The layout of the various payload experiments and support systems including power, VCO and Transmitter decks may be seen in Figure 7.

The various VCO assignments for the prime experiments, support instrumentation, housekeeping, etc. is illustrated in Table I. A total of 10 standard IRIG channels were used. In addition as an extra high frequency (channel H) VCO for the electric field experiment was required to support the bandwidth requirement of this particular experiment.

Table II provides a description of the commutator assignments. Figure 8 provides a complete payload system electrical diagram while Figure 9 represents the overall mechanical assembly.

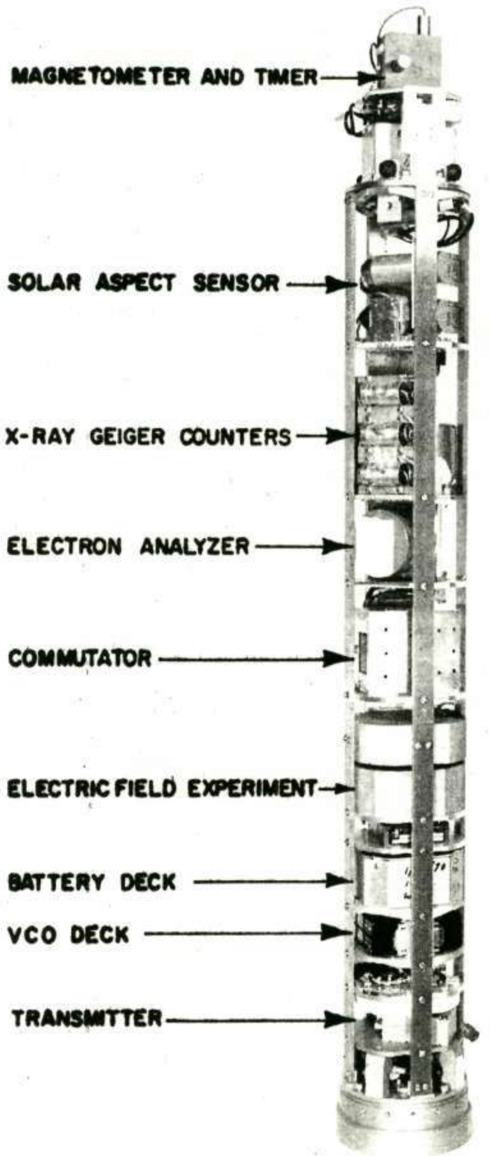

Figure 7. Nike-Apache 14.456, 14.457 including solar X-ray, electric field, and epithermal electron experiments.

TABLE I

VCO CHANNEL ASSIGNMENTS

Channel		Center Freq. (Hz)	Deviation (Hz)	Nom. Freq. Response MI = 5 (Hz)
9	Longitudinal Magnetometer	3,900	293	59
10	Roll Magnetometer	5,400	405	81
11	Solar Aspect	7,350	551	110
12	Electron Analyzer	10,500	788	160
13	Electric Field	14,500	1,088	330
15	Electric Field	30,000	2,250	450
16	Commutator	40,000	3,000	600
17	X-ray (Al) 8-20Å	52,500	3,938	790
18	X-ray (Be) 1-8Å	70,000	5,250	1,050
19	X-ray (Mylar) 44-60Å	93,000	6,975	1,395
H	Electric Field	165,000	24,750	4,950

TABLE II

COMMUTATOR ASSIGNMENTS

Segment		Segment	
1	0 Volt	16	BARO MON
2	5 Volt	17	EEA1
3	2.5 Volt	18	TIMER No. 1
4	CH 1	19	DOOR RELEASE
5	CH 2	20	INT & BATT MON
6	CH 3	21	INT & BATT MON
7	CH 4	22	EEA2
8	CH 5	23	EEA1
9	+ 15V	24	TIMER NO. 2
10	- 15V	25	DOOR RELEASE
11	ANT LENGTH	26	EEA2
12	DC x 1/4+	27	EEA1
13	DC x 1/4-	28	BARO MON
14	DC x 1	29	5 Volts
15	DC x 5	30	5 Volts

Page intentionally left blank

Page intentionally left blank

SECTION IV

FIELD OPERATIONS

In early February, 1970 the payloads were delivered to the Rocket Sounding Branch, NASA Goddard Space Flight Center, for integration, environmental and TM tests. Door deployment under spin conditions was demonstrated; in addition, the payload was spin balanced. A class C magnetic calibration required in connection with the electric field measurement was performed by placing the payloads in the Goddard Space Flight Center magnetic coil facility.

At the flight readiness and review meeting the following items were considered. The temperature dependence of the transmitter power output and frequency stability were presented and considered satisfactory. The voltage breakdown tests for both the epithermal electron and X-ray packages were discussed.

With the completion of testing the two payloads were transported directly to Wallops Island. On 17 February the project scientist attended a general planning meeting at Wallops Island to assist in the countdown, RFI and dress rehearsal preparations. Two additional GCA personnel arrived at Wallops Island on 18 February to perform vertical checks, RFI and full dress rehearsal for the 14.456 and 14.457 flights.

In the first week of March, final vehicle preparations were accomplished, horizontal and vertical tests, as well as complete countdown dress rehearsals were conducted. The photograph shown in Figure 10 displays one of the payloads for the launcher being readied for launch.

On 6 March the certification 14.456 flight was launched at 18.36:30 GMT at an azimuth of 155^{o} south and an 83^{o} AE. This launch time was based on the condition that the eclipse rocket which would be launched on the subsequent day enter the totality zone at or very near apogee at 185 km. By launching the certification round for a solar angle similar to the eclipse flight, valid comparison could be made in view of the similar atmospheric geometries.

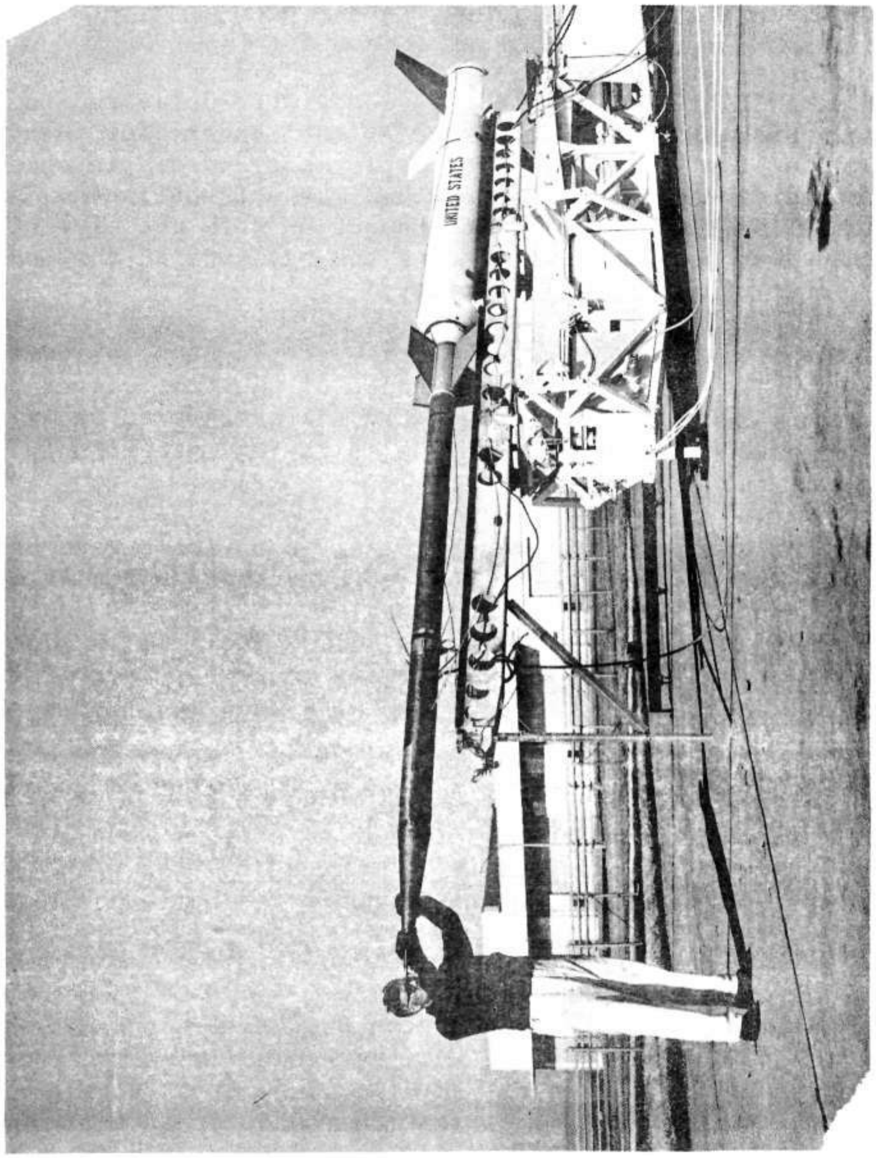

Figure 10. X-ray payload

SECTION V

SCIENTIFIC RESULTS*

The scientific results obtained in the program were presented at the Eclipse Symposium held in Seattle, Washington in June, 1971. Later a more complete paper was prepared and submitted for publication in the Journal of Atmospheric and Terrestrial Physics, Vol. 34, pp. 613-620, 1972. This paper is reproduced herein and presents the scientific results obtained.

Rocket Observations of Solar X-rays During the Eclipse of 7 March 1970

A. Introduction

Soft X-rays in the wavelength range 1-100Å are a source of ionization in the daytime D- and E-regions. The shorter wavelengths are probably not important except during a solar flare, while the longer wavelengths contribute significantly at all times. When the Sun is eclipsed the relative importance of the coronal and chromospheric radiations changes. A knowledge of the residual fluxes of soft X-rays becomes important in interpreting the variation in electron density observed during the eclipse.

Results are presented from six rocket flights. Three X-ray detectors were included in one type of payload. Two of these were flown, one 24 hours before the eclipse and the other at totality. The second type of payload carried a single detector. One of these was launched on the morning before the eclipse and three during and shortly after totality. The two launches which preceded the eclipse obtained measurements of the ambient X-ray flux, while the remaining four flights determined the residual flux in totality.

B. Experimental Details

Simple detectors are available which measure the solar flux at three representative bands of wavelength. These are Geiger counters with thin windows of different materials: beryllium for 2-8Å; aluminum for 8-20Å; and Mylar for 44-60Å (Ref. 1). The counters used in the present experiment are fabricated from stainless steel. The wall thickness is 5×10^{-2} cm, the diameter 2.5 cm, and the length 7.6 cm. They are filled with neon at a pressure of 0.5 atmosphere and with 1 percent of isobutane added as a quenching agent. The window diameters are selected to give an expected counting rate, above the absorbing region of the atmosphere,

*Paper authored by C. A. Accardo, L. G. Smith and G. A. Pintal.

of about 10^4 sec^{-1}. The window areas are made large so that the absorption profiles in the three wavelength bands can be obtained. This serves to confirm the wavelength response of the counters and gives an indication of the energy spectrum of the incident radiation.

The signals from the Geiger counters represent a very large dynamic range. In order to present this information on the FM/FM telemetry of the payload the following system is used. Each pulse from the counter is shaped using a one-shot multivibrator, which gives a square pulse of fixed amplitude and duration. A staircase generator is used as a digital-to-analog converter. It consists of a scale-of-32 combined with an adding circuit. The sensitivity is such that 32 pulses produce a 5-V signal, appropriate to the input requirement of the subcarrier-oscillator. Each return to zero represents 32 pulses and yet individual pulses can easily be counted.

The appearance of the telemetered signal from the three counters included in the payload of Nike Apache 14.457 is illustrated in Figure 11. This represents one 'look' at the Sun as the rocket spins with a revolution period of 0.53 sec. The view of the detectors is limited by the width of the opening in the payload housing. The same arrangement of detectors is used in Nike Apache 14.456, launched at the time of the eclipse but on the preceding day, 6 March 1970.

Geiger counters for the 44-60Å band are included in four additional payloads, Nike Apaches 14.435-14.438. The arrangement is identical with that of the two payloads just described except in two details. Because of telemetry limitations the signal is time-shared on IRIG Channel 19 with the output of a solar aspect sensor. In addition a slit is used to define the view of the counters. The appearance of the telemetry record on these four flights is shown in a companion paper describing solar UV observation (Figure 2, Ref. 2).

The count rate, determined at the center of each 'look,' is corrected for the deadtime of the counters. The deadtime was measured by the oscillographic method at a low count rate and checked at high count rates by the superposition-of-sources method.

C. Observations

Eclipse circumstances.- Nike Apache 14.457 was launched at 1836:30 UT on 7 March 1970 from Wallops Island, Virginia (37.84°N, 75.58°W). The eclipse circumstances are represented in Figure 12. The points marked along the plot of altitude against time show the percentage of the area of the solar disc visible at the position of the rocket. The rocket enters totality at 1839:44 UT at an altitude of 191 km on ascent. Exit occurs at 1841:34 UT at an altitude of 163.5 km on descent. The figure

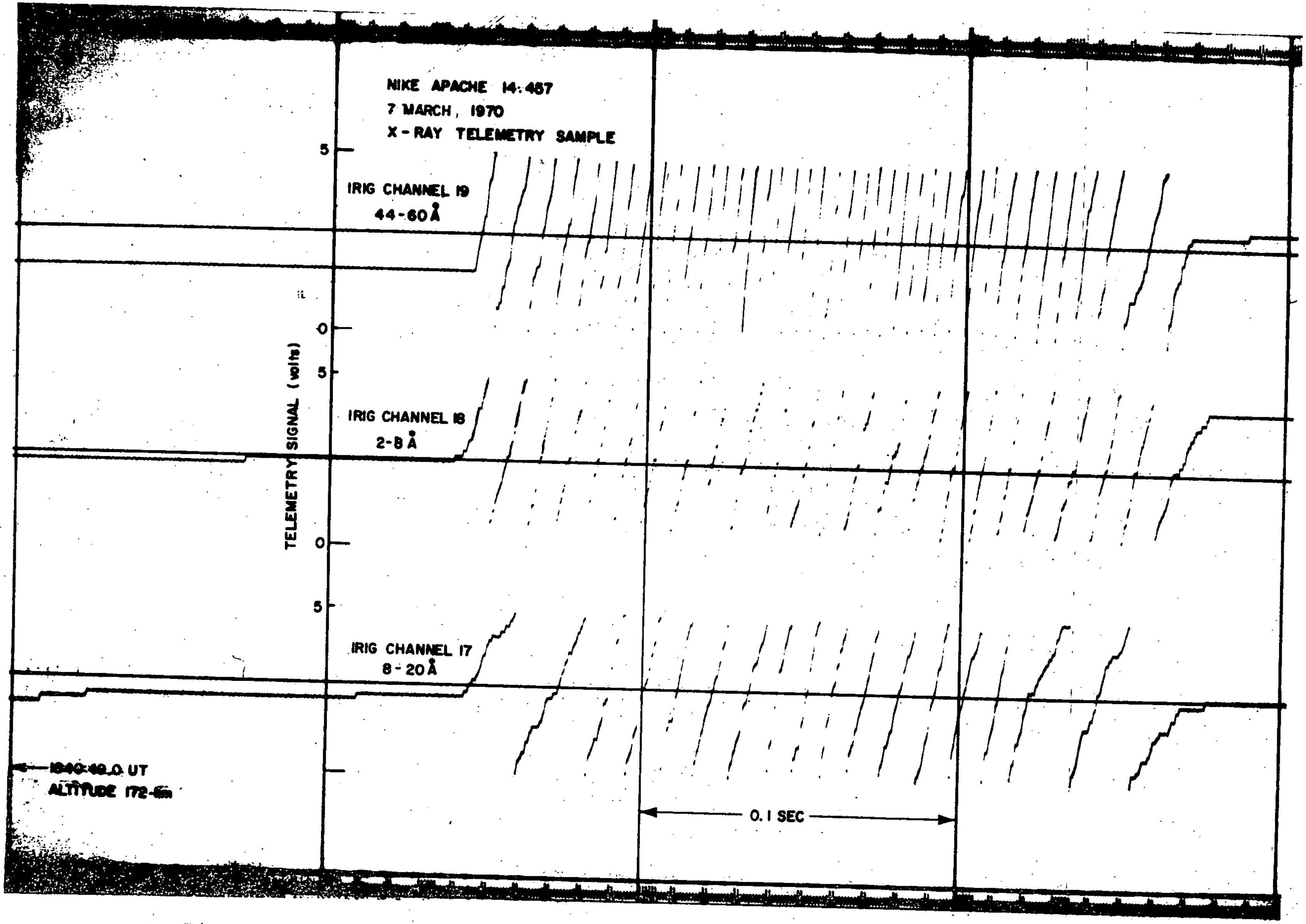

Figure 11. Section of telemetry record showing method of presenting data from the three Geiger counters.

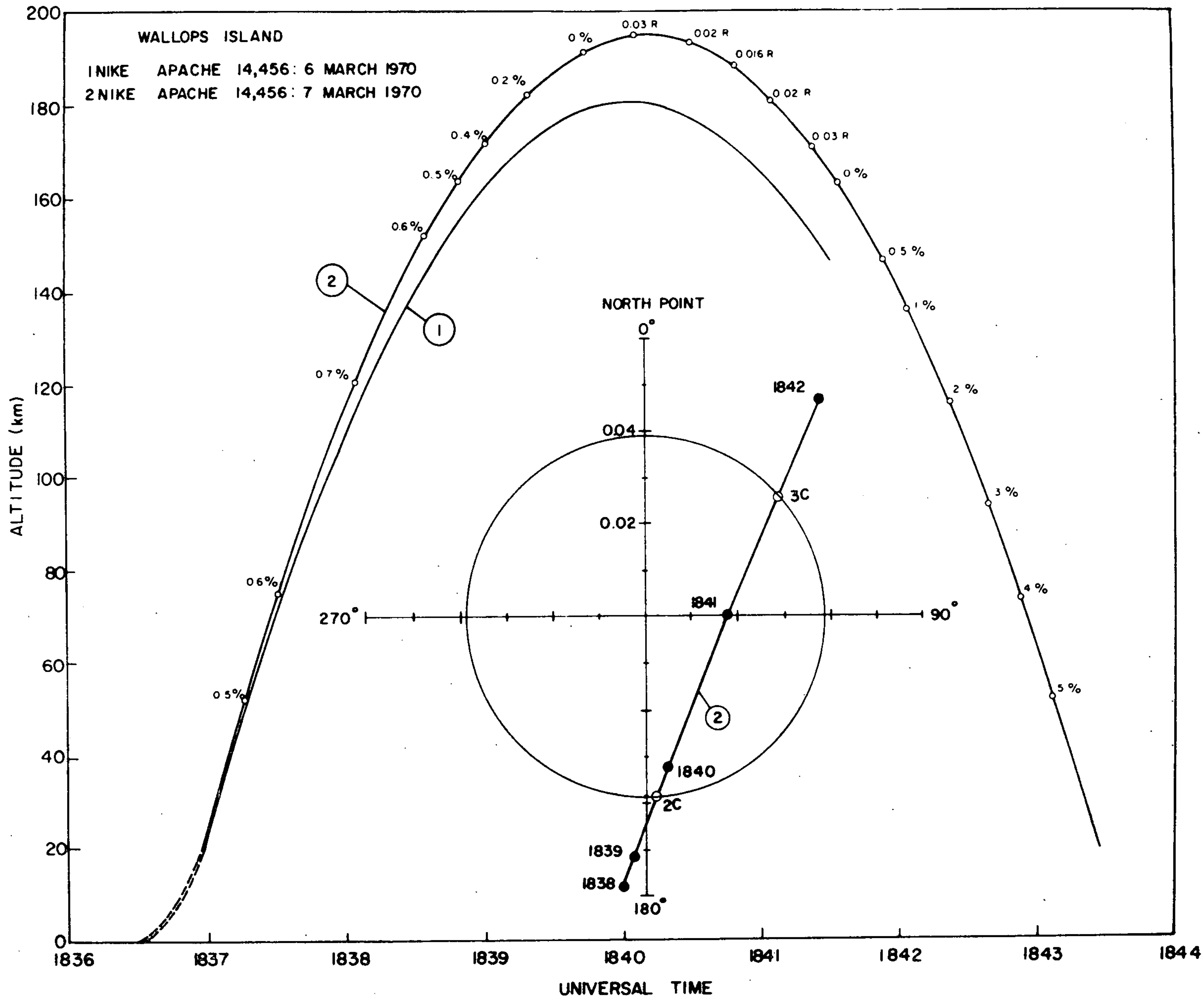

Figure 12. The altitude of the rockets as a function of time. The eclipse circumstances for Nike Apache 14.457 are also shown. See text for explanation.

also includes a plot of the apparent locus of the center of the Moon relative to that of the Sun, measured from the North Point of the Sun. The unit of distance in this plot is solar radius. This distance is also indicated on the plot of altitude against time. The rocket is closest to the center of the umbra at 1840:49 UT at an altitude of 188 km. The positions of second and third contact are, respectively, 357^o and 228^o each of the North Point, diametrically opposite the position of the center of the Moon at these times.

The altitude of Nike Apache 14.456 launched at 1836:30 UT on 6 March 1970 is also shown in Figure 12 for the period that data are available.

The eclipse circumstances of Nike Apaches 14.436, 14.437 and 14.438 are described in Reference 2 and are also represented in Reference 3. The first two rockets launched at 1837:10 UT and 1838:00 UT, intercepted the umbra. The last was launched at 1840:40 UT, shortly after third contact. Nike Apache 14.435 was launched at 1545:00 UT on the morning of the eclipse. This time was selected to give the same solar zenith angle (47^o) as at the time of mid-eclipse, in the afternoon.

Absorption profiles.- The profiles of 2-8Å flux expressed as a percentage of the incident flux are shown in Figure 13. For Nike Apache 14.456 the count rate above 96 km is very large and the dead-time correction unreliable. The count-rate corresponding to the incident flux is obtained by extrapolation, using the profile obtained from Nike Apache 14.457.

The theoretical profiles in this figure assume a spectral distribution appropriate to a black-body at temperatures of 2×10^6 °K, 1×10^6 °K and 5×10^5 °K. Absorption coefficients taken from Reference 4 and atmospheric density from 1965 CIRA are used in these calculations. The observations can be represented by the theoretical profile for 2×10^6 °K.

The profiles of 8-20Å flux expressed as a percentage of the incident flux are shown in Figure 14. The theoretical profiles are again calculated for 2×10^6 °K, 1×10^6 °K and 5×10^5 °K. Recently revised values of the mass absorption coefficients of aluminum have been used in these calculations. In this case the observed profiles are best represented by the theoretical profile for 1×10^6 °K.

The absorption profiles of 44-60Å are shown in Figure 15. Data from five rockets are included; Nike Apache 14.438 also carried a 44-60Å Geiger counter but the data are excluded on the basis of an anomalous absorption profile. Theoretical profiles have been calculated at the same three temperatures as for the other wavelength bands. The profile for 5×10^5 °K is shown in the figure. The profiles for 2×10^6 °K and 1×10^6 °K are not significantly different from the one shown: this is because the wavelength range is relatively small and falls close to the

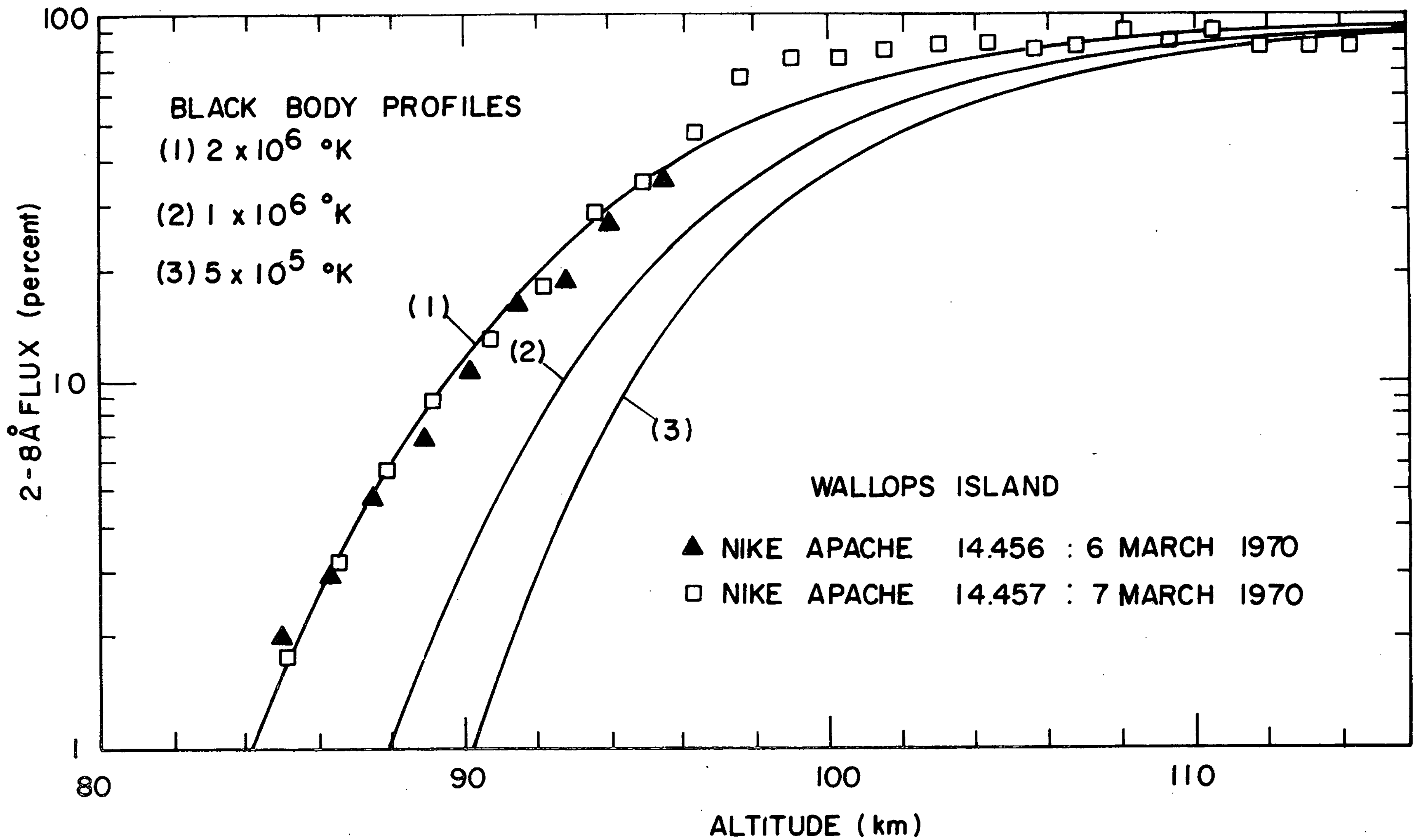

Figure 13. Observed absorption profiles of 2-8Å flux compared with theoretical profiles.

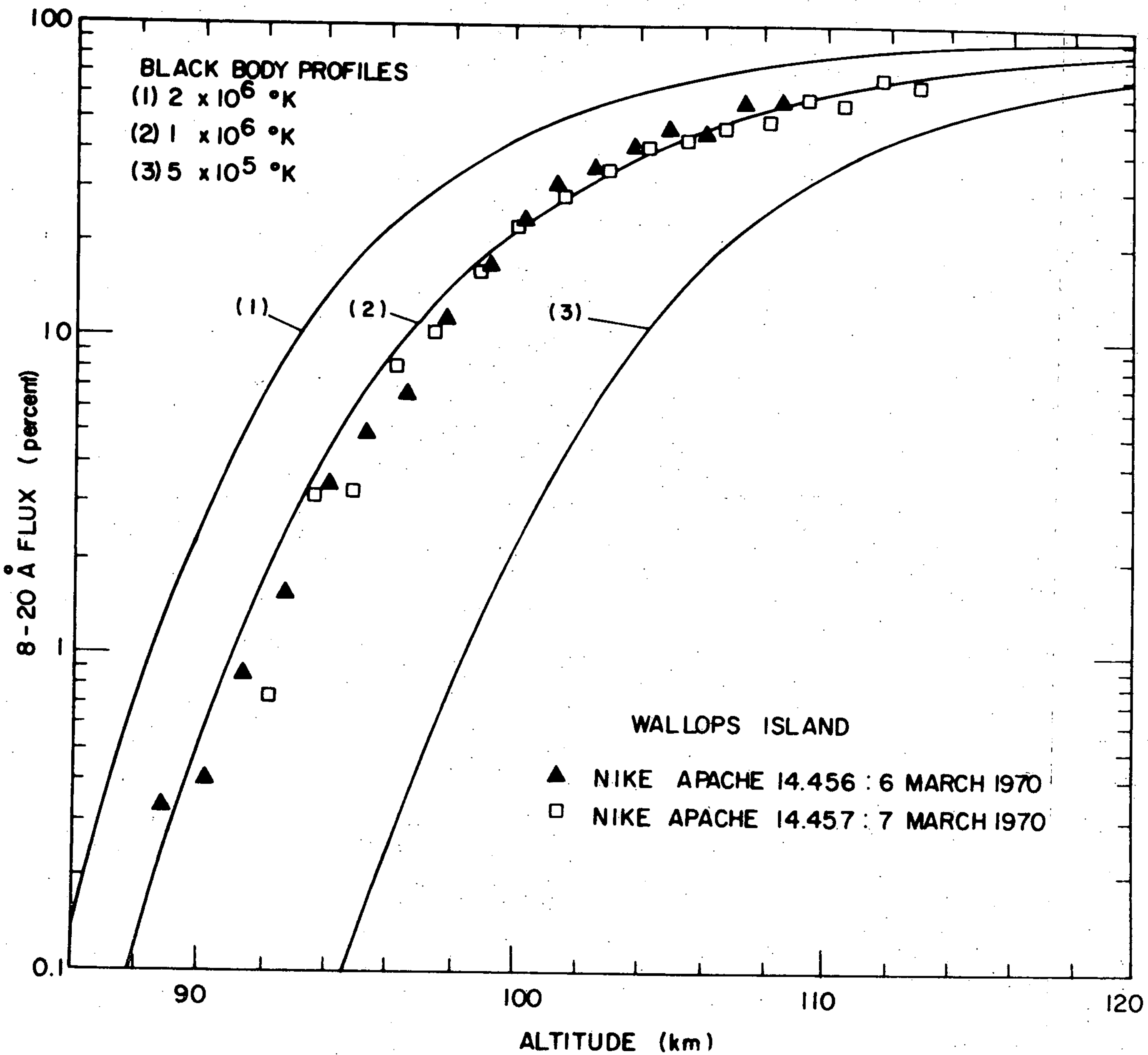

Figure 14. Observed absorption profiles of 8-20Å flux compared with theoretical profiles.

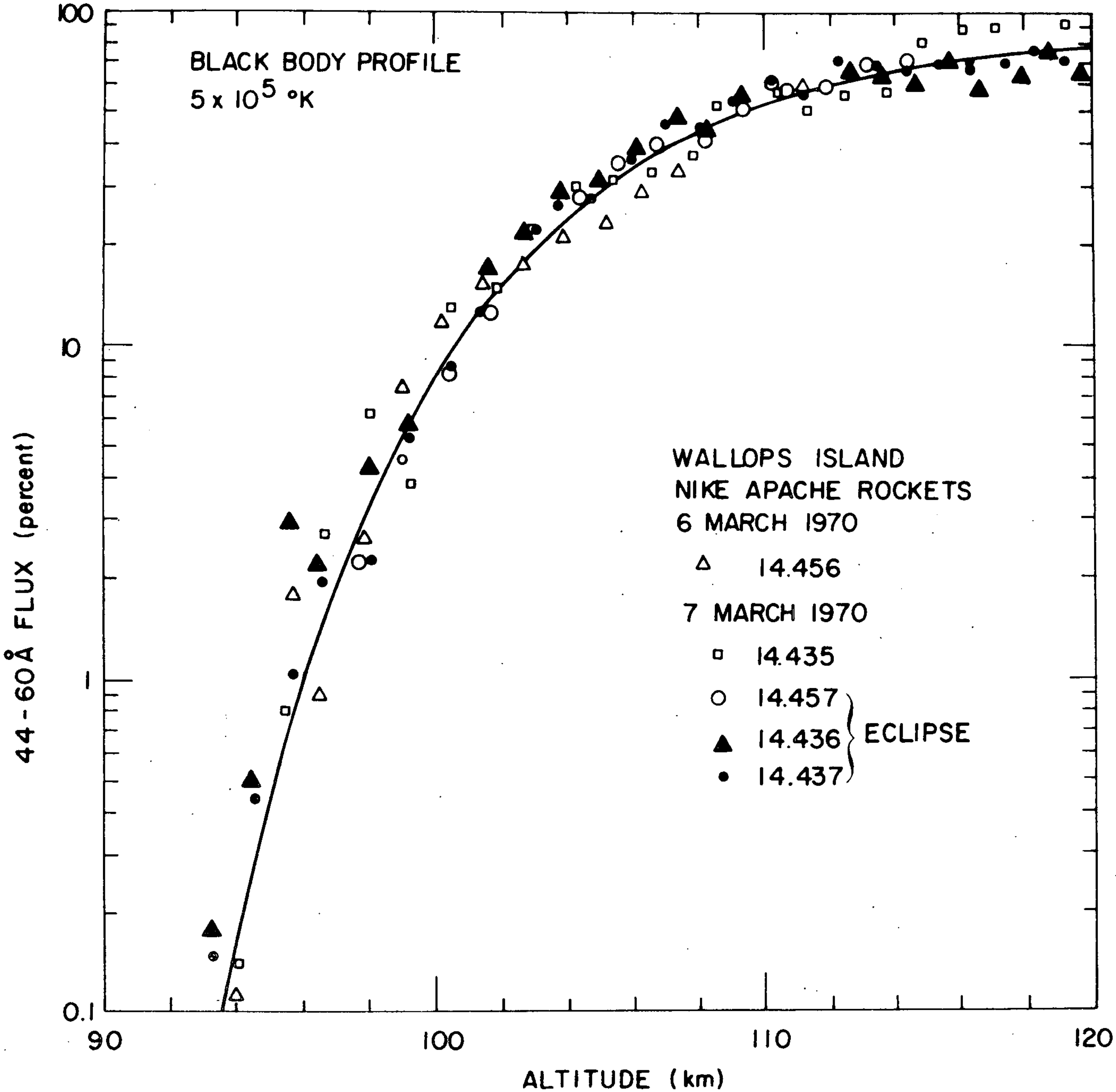

Figure 15. Observed absorption profiles of 44-60Å flux compared with theoretical profiles.

peak of the black-body energy distribution. In any case the representation of the energy distribution by a black-body temperature is somewhat artificial, especially when the source is a line spectrum, as is now established for 44-60Å. The convention of representing the energy distribution by a temperature is useful, however, for comparing with data from other broad-band detectors.

Incident flux.- The observations of the incident flux of soft X-rays measured in the three bands of wavelength are given in Table III. This also summarizes for each detector specifications of the window material, its thickness and area. The window areas for observations during the eclipse are larger by a factor of about 6 than those used for the uneclipsed sun. The columns give, in order, the Nike Apache identification number, the launch time, the observed count rate (corrected for deadtime) and the incident flux in energy units. The count rate for the 2-8Å detector of 14.456 is obtained by extrapolation from the absorption profile.

The conversion factor relating the incident flux to the corrected count rate is calculated from the physical constants of the detector and the energy spectrum of the incident radiation. The values of flux given in the table use the black-body spectrum appropriate to the temperature established from the absorption profile. These are, respectively, 2×10^6 °K for the 2-8Å flux, 1×10^6 °K for the 8-20Å flux and 5×10^5 °K for the 44-60Å flux. Additional values, in parentheses in the table, have been computed for the 8-20Å flux using a temperature of 2×10^6 °K.

Data for the 2-8Å and 8-20Å bands are available from SOLRAD 9 for comparison with the uneclipsed sun observations on 6 March 1970. The flux in these bands, both calculated on the basis of a temperature of 2×10^6 °K, are:

2-8Å	2.0×10^{-3} erg cm^{-2} sec^{-1}
8-20Å	3.4×10^{-2} erg cm^{-2} sec^{-1}

Thus there is excellent agreement at 8-20Å and fair agreement at 2-8Å. In the latter case it is likely that the rocket value is in error because of the uncertainty in the extrapolation of the count rate.

The rocket data have been examined to determine whether there is any change in flux as the limbs of the Sun are covered and uncovered. There is no clear evidence of any change greater than the uncertainty of the measurement (about 20 percent) in each of the three bands. There is no evidence of the large variation in 2-8Å flux with changing circumstances reported in Reference 5.

TABLE III

SOFT X-RAY OBSERVATIONS

(a) 2–8 Å: Beryllium $5{\cdot}1 \times 10^{-3}$ cm			
Full sun: $2{\cdot}03 \times 10^{-1}$ cm^2 aperture			
14.456	1836:30 UT*	$5{\cdot}8 \times 10^4$ sec^{-1}	$2{\cdot}6 \times 10^{-3}$ erg cm^{-2} sec^{-1}
Eclipsed sun: $1{\cdot}20$ cm^2 aperture			
14.457	1836:30 UT	$8{\cdot}0 \times 10^3$ sec^{-1}	$5{\cdot}7 \times 10^{-5}$ erg cm^{-2} sec^{-1}
(b) 8–20 Å: Aluminum $1{\cdot}3 \times 10^{-3}$ cm			
Full sun: $2{\cdot}85 \times 10^{-2}$ cm^2 aperture			
14.456	1836:30 UT*	$1{\cdot}5 \times 10^4$ sec^{-1}	$2{\cdot}7 \times 10^{-1}$ erg cm^{-2} sec^{-1} ($3{\cdot}5 \times 10^{-2}$ erg cm^{-2} sec^{-1})†
Eclipsed sun: $2{\cdot}3 \times 10^{-1}$ cm^2 aperture			
14.457	1836:30 UT	$6{\cdot}3 \times 10^3$ sec^{-1}	$1{\cdot}6 \times 10^{-2}$ erg cm^{-2} sec^{-1} ($2{\cdot}05 \times 10^{-3}$ erg cm^{-2} sec^{-1})†
(c) 44–60 Å: Mylar $6{\cdot}4 \times 10^{-4}$ cm			
Full sun: $2{\cdot}03 \times 10^{-3}$ cm^2 aperture			
14.456	1836:30 UT*	$1{\cdot}5 \times 10^4$ sec^{-1}	$1{\cdot}8 \times 10^{-1}$ erg cm^{-2} sec^{-1}
14.435	1545:00 UT	$1{\cdot}4 \times 10^4$ sec^{-1}	$1{\cdot}5 \times 10^{-1}$ erg cm^{-2} sec^{-1}
Eclipsed sun: $1{\cdot}27 \times 10^{-2}$ cm^2 aperture			
14.457	1836:30 UT	$1{\cdot}5 \times 10^4$ sec^{-1}	$2{\cdot}8 \times 10^{-2}$ erg cm^{-2} sec^{-1}
14.436	1837:10 UT	$1{\cdot}4 \times 10^4$ sec^{-1}	$2{\cdot}6 \times 10^{-2}$ erg cm^{-2} sec^{-1}
14.437	1838:00 UT	$1{\cdot}25 \times 10^4$ sec^{-1}	$2{\cdot}4 \times 10^{-2}$ erg cm^{-2} sec^{-1}

* 6 March 1970, all others 7 March 1970.
† 2×10^6 °K.

Residual flux.- The data from SOLRAD 9 show that the flux from the uneclipsed sun in the 2-8Å and 8-20Å bands is less at the time of the eclipse measurements than it had been 24 hours earlier. The fluxes, both calculated for a temperature of 2 x 10^6 °K, are, at the time of mid-eclipse:

2-8Å	1.1×10^{-3} erg cm^{-2} sec^{-1}
8-20Å	2.9×10^{-2} erg cm^{-2} sec^{-1}

Taking the ratio of the flux from the eclipsed sun, from the rocket observation given in Table III, to the flux from the uneclipsed sun, measured simultaneously from the satellite, we obtain the following values of the residual flux, expressed as a percentage of that from the uneclipsed sun:

2-8Å	$(5.7 \times 10^{-5}/1.1 \times 10^{-3})$	5.2 percent
8-20Å	$(2.05 \times 10^{-3}/2.9 \times 10^{-2})$	7.1 percent

For 44-60Å radiation, no simultaneous observation of the flux from the uneclipsed sun is available. This radiation is less variable in intensity than are the shorter wavelengths. Accordingly, it is with reasonable confidence that we compare the flux observed during the eclipse (average of three measurements) with the flux from the uneclipsed sun (average of two measurements) and obtain as the residual flux:

44-60Å	$(2.6 \times 10^{-2}/1.65 \times 10^{-1})$	15.8 percent

It appears that the residual flux in the 8-20Å band has not previously been measured during totality. Mandelshtam et al. (Ref. 6) have reported a measurement of flux in the 2-8Å band during the eclipse of 15 February 1961. This was compared with predictions based on a model of Elwert (Ref. 7) and found to be in good agreement. The residual flux in the 44-60Å band during the eclipse of 12 October 1958 has been reported by Kreplin (Ref. 1) as being between 10 and 13 percent of that of the uneclipsed sun. Smith et al. (Ref. 8) found during the eclipse of 20 July 1963, at a time when 6 percent of the disc was visible, a residual flux of 19 percent in the 44-60Å band.

D. Discussion

E-region.- The ionosonde at Wallops Island shows the value of f_oE to be 2.15 MGz at mid-eclipse (1839 UT), corresponding to an electron density of 5.73×10^4 cm^{-3}. On the morning of the eclipse the same solar zanith angle (47^{o}) occurred at 1545 UT (the launch time of Nike Apache 14.435). The value of f_oE at this time is 3.50 MGz corresponding to an electron density of 1.52×10^5 cm^{-3}. The same value of f_oE was recorded at 1830 UT on 6 March 1970. This value of electron density represents the condition of the ionosphere for the uneclipsed sun. The effect of this eclipse on the E-layer is to reduce the electron density to 37.7 percent of the normal value. If, as we believe, the recombination coefficient at the altitude of the E-layer (110 km) is greater than 1×10^{-7} cm^3 sec^{-1}, the layer remains in equilibrium with the incident radiation, and since the ionizing radiation is proportional to (electron density)^2, we deduce that radiation is reduced to 14.2 percent of its normal value. This supports the earlier eclipse observation (Ref. 8) that the radiation maintaining the E-layer appears to vary porportionately with the 44-60Å radiation, a coronal radiation. It is not yet explained how this can be reconciled with the role of chromospheric radiations such as Lyman-β (1026Å) in the formation of the E-layer.

D-region.- At an altitude of 80 km the D-layer is principally formed by ionization of nitric oxide by solar Lyman-α (1216Å). X-rays at wavelengths shorter than 10Å are not important except during periods of solar flare activity. Galactic cosmic rays are another source of ionization but normally insignificant.

The relative importance of these sources during totality will now be evaluated for an altitude of 80 km. Adapting calculations given by Swider (Ref. 4) we find that the ion production rate in totality due to the measured 2-8Å flux is 1.1×10^{-2} ion-pairs cm^{-3} sec^{-1}. For ionization of nitric oxide by Lyman-α in totality, we use the concentration of nitric oxide determined by Meira (Ref. 9), 2×10^7 cm^{-3}, and the Lyman-α flux from Smith (Ref. 2) 1×10^9 photons cm^{-2} sec^{-1}. This gives a production rate of 4×10^{-2} ion-pairs cm^{-3} sec^{-1}. The production rate for galactic cosmic rays is about 4×10^{-3} ion-pairs cm^{-3} sec^{-1}. It thus appears that the total production rate at 80 km in totality from these three sources is 5.5×10^{-2} ion-pairs cm^{-3} sec^{-1} of which the major part is ionization of nitric oxide by Lyman-α.

Acknowledgement - The research described here has been supported by the National Aeronautics and Space Administration. The SOLRAD 9 data were supplied by R. W. Kreplin.

ACKNOWLEDGEMENTS

The success of the program was made possible through the efforts of many people. In particular the author expresses his gratitude to Dr. Nelson Maynard, NASA, Dr. Gerald Sharp, Lockheed Corp. Also the efforts of Mr. Frank Wanko, Lorenzo Johnson, William Aman and Gerald Pintal were instrumental in the overall success of the program. Finally, the assistance and collaboration of Dr. Leslie Smith, a former colleague, and presently at the University of Illinois are greatly appreciated.

REFERENCES

1. Kreplin, R.W., Annls. Geophys. 17, 314 (1961).

2. Smith, L.G., J. Atmosph. Terr. Phys. 34, 601 (1972).

3. Mechtly E.A., Sechrist, C.F. and Smith, L.G., J. Atmosph. Terr. Phys. 34, 641 (1972).

4. Swider, W., Rev. Geophys. 7, 573 (1969).

5. Hall, J.E., Dickinson, P.H.G. and Hall, A.J., Nature, London 226, 1105 (1970).

6. Mandelshtam, S., Vasilyev, B., Voron'ko, J., Tindo, I., and Shurygin, A., Space Research III (edited by W. Priester), p. 822. North-Holland, Amsterdam (1963).

7. Elwert, G., J. Atmosph. Terr. Phys. 12, 187 (1958).

8. Smith, L.G., Accardo, C.A., Weeks, L.H., and McKinnon, P.J., J. Atmosph. Terr. Phys. 27, 803 (1965).

9. Meira, L.G., J. Geophys. Res. 76, 202 (1971).

APPENDIX A

COMPUTER PROGRAM FOR THE ECLIPSE OF 7 MARCH 1970

A computer program designed primarily for use with a rocket trajectory has been prepared to calculate the circumstances of the 7 March 1970 total solar eclipse. The equations for the program are found in the Explanatory Supplement to the Ephemeris, 1961. The Besselian elements contained in the program are tabulated in the American Ephemeris and Nautical Almanac, 1970. These are reproduced in Table A-1. The values for 1830 ephemeris time are used in the program.

The program has been verified using data from the US Naval Observatory Circular No. 125. An example of the input and output data format is attached.

This program was developed by R. V. Sillars, with modifications by L. G. Smith and G. A. Pintal.

.TYPE ECLIP2.FOR

ECLIPSE OF 7 MARCH 1970

ECLIP2.FOR

```
  REFERENCE 1830UT
        IMPLICIT DOUBLE PRECISION (A-H,O-Z)
      PI=3.1415927
      SX=60.0
      DR=0.017453293
      F2=0.99330546
      U0=94.72688*DR
      D0=DATAN(-0.091063/0.995845)
      TF1=0.004710
      TF2=0.004687
      DUM=0.261865
      DD=0.000271
      CONTINUE
      READ(1,94) M
      TH=18.0
      TM0=30.0
      X0=0.220318
      X1=0.304554
      Y0=0.628851
      Y1=0.674683
      EL10=0.539479
      DEL1=0.000008
      EL20=-0.006832
      DEL2=0.000007
      DX=(X1-X0)*6.0
      DY=(Y1-Y0)*6.0
      DO 50 J=1,M
        READ(1,93)TM,TS,ALT,FLAT,FLONG
      ALT=ALT/1000.
      SPHI=DSIN(FLAT*DR)
      CPHI=DCOS(FLAT*DR)
      Q=DSQRT(1.0/(CPHI**2+F2*(SPHI**2)))
      PS=(F2*Q+0.15677940E-03*ALT)*SPHI
      PC=(Q+0.15677940E-03*ALT)*CPHI
      TN=TM+TS/SX+0.645
      TE=TH+TN/SX
      X=X0+(DX/SX)*(TN-TM0)
      Y=Y0+(DY/SX)*(TN-TM0)
      EL1=EL10+0.1*DEL1*(TN-TM0)
      EL2=EL20+0.1*DEL2*(TN-TM0)
      D=D0+DD*(TE-18.5)
      SD=DSIN(D)
      CD=DCOS(D)
      UM=U0+DUM*(TE-18.5)
      HH=UM-FLONG*DR-0.0028 1435
      SH=DSIN(HH)
      CH=DCOS(HH)
      XI=PC*SH
      ETA=PS*CD-PC*SD*CH
      ZET=PS*SD+PC*CD*CH
      DXI=DUM*PC*CH
      DETA=DUM*XI*SD-ZET*DD
```

```
U=X-XI
DU=DX-DXI
V=Y-ETA
DV=DY-DETA
EN2=DU**2+DV**2
EN=DSQRT(EN2)
DEL=(U*DV-DU*V)/EN
DDD=U*DU+V*DV
ELL1=EL1-ZET*TF1
ELL2=EL2-ZET*TF2
EM2=U*U+V*V
EM=DSQRT(EM2)
ELLP=ELL1+ELL2
S=(ELL1-ELL2)/ELLP
AB=2.0*EM/ELLP
TAU=-DDD*SX/EN2
CPSI=SX*DSQRT(ELL1**2-DEL**2)/(ELL1*EN)
TAU1=TAU-ELL1*CPSI
TAU2=TAU+ELL2*CPSI
AQ=DATAN(U/V)
IF(V) 41,42,42
AQ=PI+AQ
GO TO 44
IF(U) 43,44,44
AQ=2.0*PI+AQ
AQ=AQ/DR
AC=DATAN(XI/ETA)
IF(ETA) 45,46,46
AC=PI+AC
GO TO 48
IF(XI) 47,48,48
AC=2.0*PI+AC
AC=AC/DR
AN=DATAN(DU/DV)
IF(DV) 31,32,32
AN=PI+AN
GO TO 34
IF(DU) 33,34,34
AN=2.0*PI+AN
AN=AN/DR
AV=AQ-AC
IF(AV) 49,51,51
AV=AV+360.0
AP=22.35-0.01*(TH+1.0)
AQP=AQ-AP
WEM=DDD/EN
WLD1=ELL1**2-DEL**2
WLD2=ELL2**2-DEL**2
IF(WLD2) 61,62,62
W2=WEM+DSQRT(WLD2)
T2=-W2*SX/EN
```

```
W1=WEM+DSQRT(WLD1)
T1=-W1*SX/EN
K=1
GO TO 65
 IF(WLD1) 63,64,64
 W1=WEM+DSQRT(WLD1)
T1=-W1*SX/EN
K=2
GO TO 65
 K=3
 IF(EM+ELL2) 11,11,12
 AR=1.0
 ARV=0.0
BB=0.0
EMM1=1.0
GO TO 30
 IF(EM-ELL1) 13,13,14
 AR=0.0
  ARV=1.0
BB=360.0
EMM1=0.0
GO TO 30
 CC=(ELL1**2+ELL2**2-2.0*EM2)/(ELL1**2-ELL2**2)
SC=DSQRT(1.0-CC**2)
C=DATAN(SC/CC)
CB=(ELL1*ELL2+EM2)/(EM*ELLP)
SB=DSQRT(1.0-CB**2)
B=DATAN(DSQRT(1.0-CB**2)/CB)
IF(CC) 21,22,22
 C=PI+C
 IF(CB) 23,24,24
 B=PI+B
 BB=360.0-2.0*B/DR
EMM1=(ELL1-EM)/ELLP
A=PI-B-C
AR=(S*S*A+B-S*SC)/PI
  ARV=1.0-AR
  TYPE 97,TM,TS,ALT,FLAT,FLONG
  TYPE 97,TAU,S,AB,EMM1,BB
  TYPE 97,AR,ARV,AQ,AV,AN
  GO TO (66,67,68),K
  TYPE 97,AC,AP,AQP,T1,T2
  GO TO 50
  TYPE 97,AC,AP,AQP,T1
  GO TO 50
  TYPE 97,AC,AP,AQP
 TYPE 90
GO TO 1
 FORMAT(1H )
 FORMAT(5F )
 FORMAT(I ,F )
  FORMAT(1X,5F11.6)
END
```

Glossary

PI	π
SX	seconds per minute; minutes per hour
DR	radians per degree
F2	[(polar radius)/(equatorial radius)]^2, Hayford's spheroid
VO	μ, in radians
DO	d, in radians, from $\tan^{-1}[(\sin d)/(\cos d)]$
TF1	$\tan f_1$
TF2	$\tan f_2$
DUM	μ', in radians per hour
DD	d', in radians per hour
M	number of trajectory points to be calculated
TH	hour, universal time
TMO	minutes, ephemeris time, of Besselian elements
XO	x, at 1830 ET
X1	x, at 1840 ET
YO	y, at 1830 ET
Y1	y, at 1840 ET
EL10	ℓ_1 (penumbra), at 1830 ET
DEL1	(ℓ_1, at 1840 ET) - (ℓ_1, at 1830 ET)
EL20	ℓ_2 (umbra), at 1830 ET
DEL2	(ℓ_2, at 1840 ET) - (ℓ_2, at 1830 ET)
TM	minutes, UT
TS	seconds, UT

ALT	altitude, in km
FLONG	longitude, in degrees, positive toward west
FLAT	latitude, in degrees, positive toward north
TAU	minutes to maximum phase
S	radius of moon (solar radii)
AB	distance between center of sun and center of moon (solar radii)
EMM1	fraction of solar diameter covered by moon
BB	degrees on the solar rim not obscured by the moon
AR	fraction of solar disk obscured
AQ	angle (degrees) to the center of the moon east of the sun's north point
AV	angle (degrees) to the center of the moon east of the sun's vertex
AN	azimuth (degrees of the eclipse axis path east of the sun's north point)
AC	the parallactic angle (degrees), the angle to the vertex east of the north point
AP	angle (degrees) of the sun's north pole east of the sun's north
AQP	angle (degrees) to the center of the moon east of the sun's north pole
TAU	minutes to maximum phase
S	radius of moon (solar radii)
AB	distance between center of sun and center of moon (solar radii)
EMM1	fraction of solar diameter covered by moon
BB	degrees on the solar rim not obscured by the moon
AR	fraction of solar disk obscured
AQ	angle (degrees) to the center of the moon east of the sun's north point

AV	angle (degrees) to the center of the moon east of the sun's vertex
AN	azimuth (degrees of the eclipse axis path east of the sun's north point)
AC	the parallactic angle (degrees), the angle to the vertex east of the north point
AP	angle (degrees) of the sun's north pole east of the sun's north point
AQP	angle (degrees) to the center of the moon east of the sun's north pole
ELL1	radius of penumbra (earth radii)
ELL2	radius of umbra (earth radii)
EM	distance (earth radii) from the observer to the eclipse axis
EN	hourly rate of change of EM
TAU1	minutes to first contact along eclipse axis path
TAU2	minutes to second contact along eclipse axis path
DEL	distance (earth radii) from the observer to the eclipse axis path
WEM	distance (earth radii) from the observer parallel to the eclipse axis path to the point of maximum phase
W1	distance (earth radii) from the observer parallel to the eclipse axis path to the penumbra (first contact)
T1	W1 in minutes
W2	distance (earth radii) from the observer parallel to the eclipse axis path to the umbra (second contact)
T2	W2 in minutes

The relation between these output values is shown schematically in Figures A-1 and A-2.

TABLE A-1

ECLIPSES, 1970

BESSELIAN ELEMENTS OF THE TOTAL ECLIPSE OF THE SUN MARCH 7

E.T.		Intersection of Axis of Shadow with Fundamental Plane		Direction of Axis of Shadow			Radius of Shadow on Fundamental Plane	
		x	y	sin d	cos d	μ	Penumbra	Umbra
h	m					°		
15	00	−1.548751	−0.333523	−0.092008	0.995758	42.21379	0.539158	−0.007152
	10	1.464521	0.287708	.091963	.995762	44.71441	.539180	.007130
	20	1.380288	0.241891	.091918	.995767	47.21503	.539202	.007109
	30	1.296054	0.196072	.091873	.995771	49.71566	.539223	.007088
	40	1.211817	0.150251	.091828	.995775	52.21628	.539243	.007068
	50	1.127577	0.104429	.091783	.995779	54.71690	.539263	.007048
16	00	−1.043337	−0.058605	−0.091738	0.995783	57.21753	0.539282	−0.007029
	10	0.959095	−0.012780	.091693	.995787	59.71815	.539300	.007011
	20	0.874852	+0.033046	.091648	.995791	62.21877	.539317	.006994
	30	0.790607	0.078873	.091603	.995796	64.71940	.539334	.006977
	40	0.706363	0.124701	.091558	.995800	67.22002	.539350	.006961
	50	0.622117	0.170529	.091513	.995804	69.72064	.539365	.006946
17	00	−0.537871	+0.216359	−0.091468	0.995808	72.22126	0.539380	−0.006932
	10	0.453625	0.262190	.091423	.995812	74.72189	.539394	.006918
	20	0.369379	0.308021	.091378	.995816	77.22251	.539407	.006905
	30	0.285134	0.353853	.091333	.995820	79.72314	.539419	.006892
	40	0.200889	0.399686	.091288	.995825	82.22376	.539431	.006880
	50	0.116645	0.445519	.091243	.995829	84.72438	.539442	.006869
18	00	−0.032402	+0.491352	−0.091198	0.995833	87.22501	0.539453	−0.006859
	10	+0.051840	0.537185	.091153	.995837	89.72563	.539462	.006850
	20	0.136080	0.583018	.091108	.995841	92.22626	.539471	.006841
	30	0.220318	0.628851	.091063	.995845	94.72688	.539479	.006832
	40	0.304554	0.674683	.091018	.995849	97.22750	.539487	.006825
	50	0.388787	0.720515	.090973	.995853	99.72813	.539494	.006818
19	00	+0.473019	+0.766347	−0.090928	0.995857	102.22875	0.539500	−0.006812
	10	0.557248	0.812177	.090883	.995862	104.72937	.539505	.006807
	20	0.641474	0.858007	.090838	.995866	107.23000	.539510	.006802
	30	0.725697	0.903835	.090793	.995870	109.73062	.539514	.006798
	40	0.809917	0.949662	.090748	.995874	112.23125	.539518	.006795
	50	0.894134	0.995488	.090703	.995878	114.73187	.539520	.006792
20	00	+0.978347	+1.041312	−0.090658	0.995882	117.23250	0.539522	−0.006790
	10	1.062555	1.087134	.090613	.995886	119.73312	.539523	.006789
	20	+1.146760	+1.132955	−0.090568	0.995890	122.23375	0.539524	−0.006788

tan f_1 0.004710
tan f_2 0.004687
μ' 0.261865 radians per hour
d' +0.000271 radians per hour

ECLIPSE CIRCUMSTANCES

Revised Printout for Program Dated 15 September 1970

OUTPUT FORMAT

TM	TS	ALT	FLAT	FLONG
TAU	S	AB	EMM1	BB
AR	ARV	AQ	AV	AN
AC	AP	AQP	T1	T2

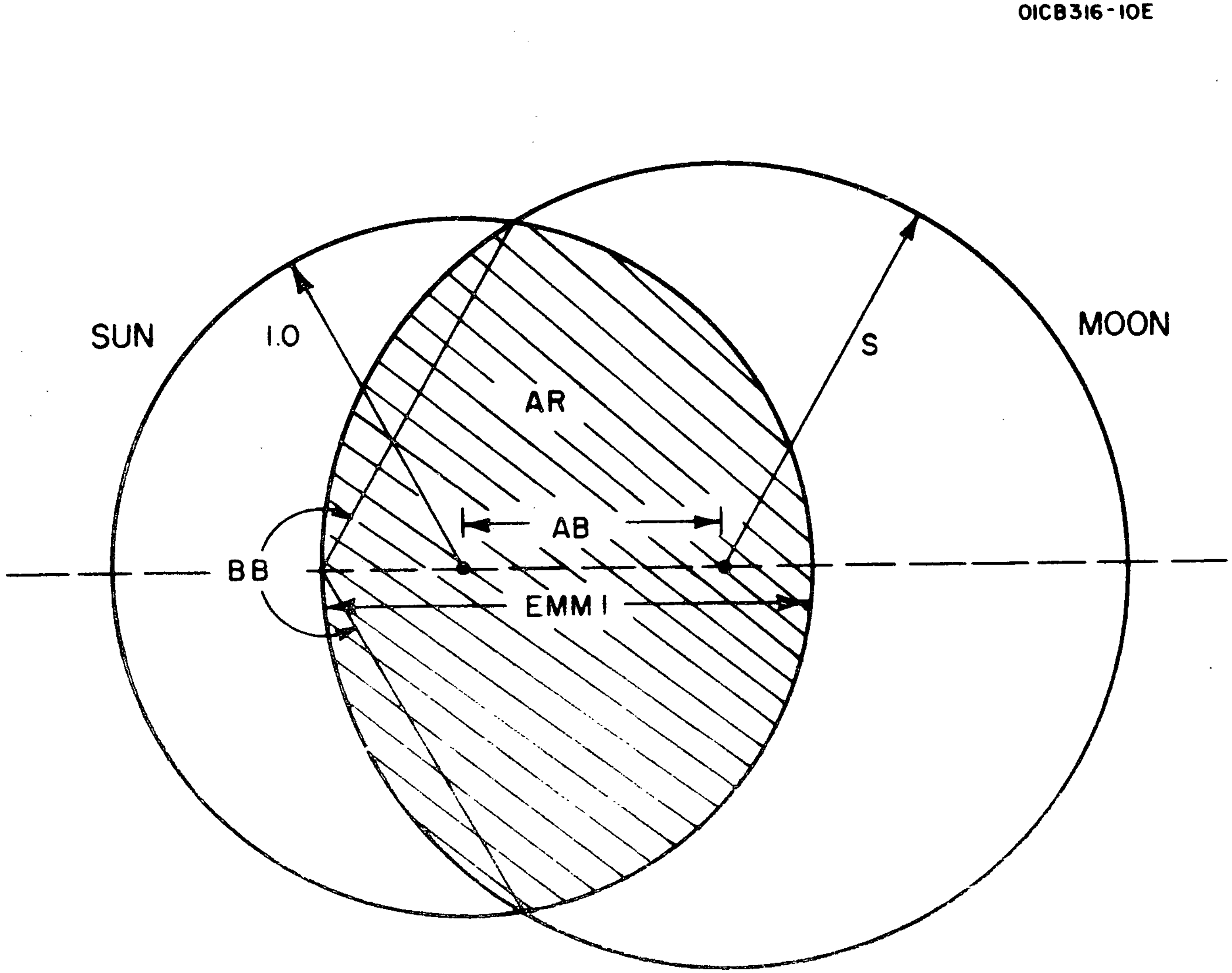

Figure A-1

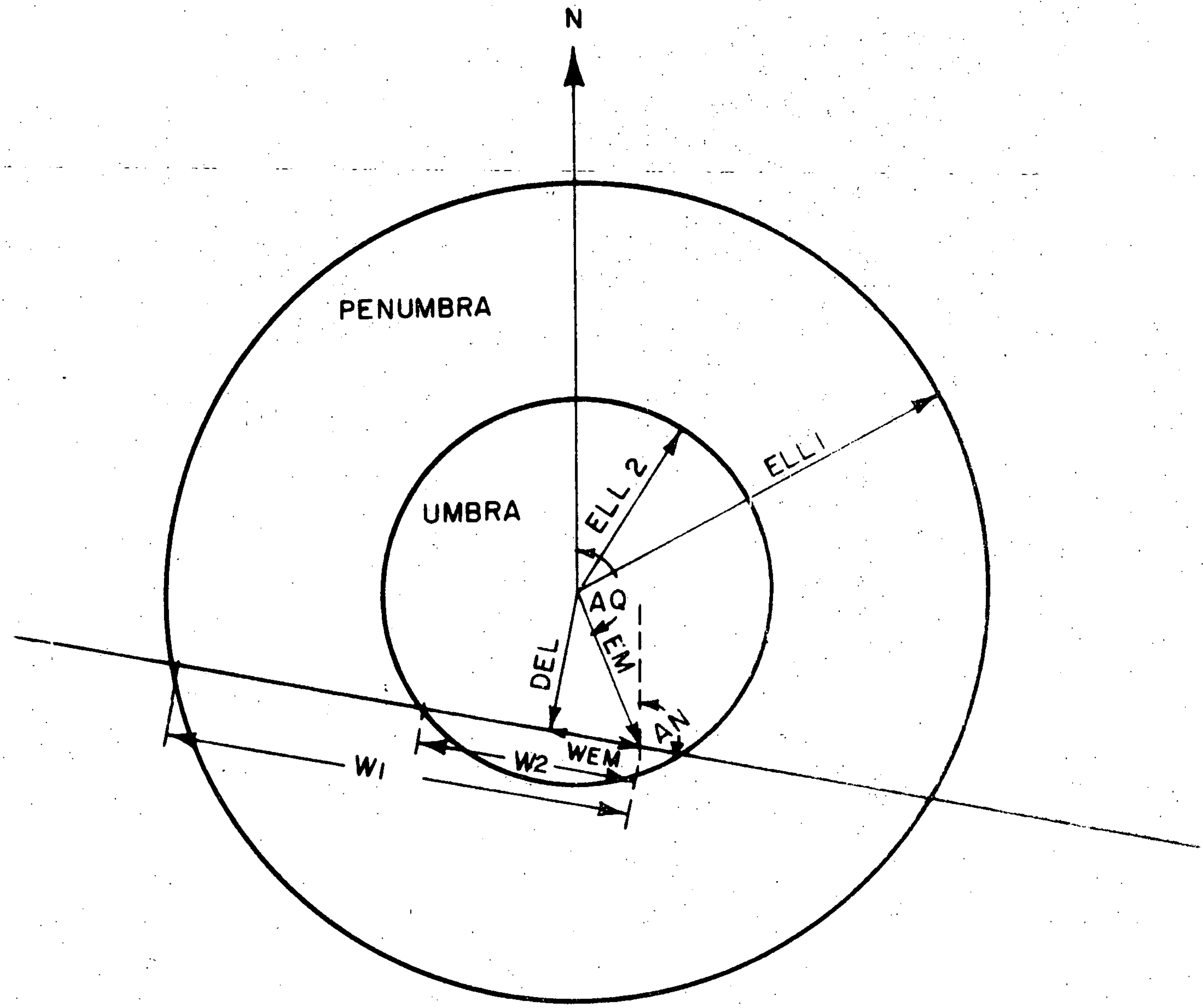

Figure A-2

14.457 Revised Trajectory

37.000000	10.000000	42.095000	37.769300	75.429701
1.370191	1.038137	0.051942	0.993098	87.517640
0.995588	0.004412	182.301550	159.391500	47.776945
22.910049	22.160000	160.141550	-75.290330	1.027296
37.000000	15.000000	50.452000	37.750800	75.420800
1.409338	1.038155	0.052924	0.992615	89.819584
0.995159	0.004841	182.788380	159.838080	47.750820
22.950299	22.160000	160.628380	-75.283366	1.124902
37.000000	20.000000	58.591000	37.733400	75.412401
1.445543	1.038171	0.053870	0.992150	91.919015
0.994738	0.005262	183.181960	160.192600	47.725538
22.989361	22.160000	161.021960	-75.278214	1.242228
37.000000	25.000000	66.446000	37.714600	75.404200
1.476145	1.038188	0.054632	0.991778	93.522963
0.994396	0.005604	183.539490	160.510300	47.700690
23.029189	22.160000	161.379490	-75.278148	1.358889
37.000000	30.000000	74.133001	37.698000	75.396900
1.504912	1.038204	0.055427	0.991388	95.137483
0.994033	0.005967	183.779960	160.713250	47.676784
23.066713	22.160000	161.619960	-75.278643	
37.000000	35.000000	81.562000	37.681401	75.389200
1.530396	1.038219	0.056116	0.991051	96.478611
0.993715	0.006285	184.000830	160.896200	47.653648
23.104630	22.160000	161.840830	-75.281373	
37.000000	40.000000	88.662000	37.662000	75.379801
1.550928	1.038234	0.056536	0.990849	97.257843
0.993523	0.006477	184.311600	161.165550	47.630904
23.146050	22.160000	162.151600	-75.288527	
37.000000	45.000000	95.534001	37.643500	75.368700
1.571084	1.038248	0.056908	0.990670	97.932127
0.993353	0.006647	184.658550	161.470060	47.609193
23.188488	22.160000	162.498550	-75.294537	
37.000000	50.000000	102.272000	37.626201	75.364901
1.580528	1.038262	0.057264	0.990499	98.565285
0.993189	0.006811	184.600740	161.377490	47.587492
23.223251	22.160000	162.440740	-75.311702	
37.000000	55.000000	108.694000	37.607100	75.358501
1.587201	1.038276	0.057406	0.990435	98.792964
0.993128	0.006872	184.666350	161.404660	47.566483
23.261700	22.160000	162.506360	-75.330618	

38.000000	5.000000	120.920000	37.573800	75.340100
1.602879	1.038301	0.057678	0.990312	99.228964
0.993010	0.006990	184.907680	161.567060	47.528001
23.340617	22.160000	162.747680	-75.360876	
38.000000	10.000000	126.706000	37.556900	75.333001
1.602797	1.038313	0.057659	0.990327	99.160821
0.993026	0.006974	184.889130	161.510840	47.509444
23.378289	22.160000	162.729130	-75.383183	
38.000000	15.000000	132.214000	37.539400	75.325401
1.598688	1.038325	0.057495	0.990415	98.825762
0.993111	0.006889	184.872030	161.455170	47.491587
23.416856	22.160000	162.712030	-75.408589	
38.000000	20.000000	137.492000	37.521901	75.317801
1.591107	1.038336	0.057234	0.990551	98.307020
0.993243	0.006757	184.826210	161.370770	47.474397
23.455440	22.160000	162.666210	-75.436592	
38.000000	25.000000	142.503000	37.503500	75.309500
1.579669	1.038346	0.056818	0.990764	97.487547
0.993448	0.006551	184.798470	161.303150	47.457820
23.495314	22.160000	162.638470	-75.467635	
38.000000	30.000000	147.288000	37.485900	75.301201
1.565479	1.038357	0.056347	0.991005	96.542148
0.993679	0.006321	184.725680	161.191020	47.442106
23.534661	22.160000	162.565680	-75.500266	1.444934
38.000000	35.000000	151.831000	37.468201	75.293000
1.547400	1.038366	0.055768	0.991299	95.360044
0.993957	0.006043	184.616460	161.042460	47.427062
23.573999	22.160000	162.456460	-75.535921	1.321592
38.000000	40.000000	156.116000	37.449301	75.284101
1.525324	1.038376	0.055025	0.991675	93.797725
0.994310	0.005690	184.530090	160.915260	47.412534
23.614833	22.160000	162.370090	-75.574892	1.207454
38.000000	45.000000	160.182000	37.430800	75.275401
1.499985	1.038384	0.054209	0.992088	92.014969
0.994691	0.005309	184.392570	160.737350	47.398731
23.655225	22.160000	162.232580	-75.616174	1.110005
38.000000	50.000000	164.051000	37.413100	75.267600
1.471112	1.038393	0.053348	0.992522	90.049339
0.995086	0.004914	184.158180	160.463940	47.385624
23.694239	22.160000	161.998180	-75.660113	1.024968

38.000000	55.000000	167.718000	37.396200	75.260201
1.439299	1.038400	0.052443	0.992979	87.878165
0.995494	0.004506	183.847900	160.115560	47.373275
23.732343	22.160000	161.687900	-75.705995	0.945420
39.000000	0.000000	171.200000	37.380500	75.253501
1.404743	1.038408	0.051519	0.993444	85.544768
0.995901	0.004099	183.434640	159.665660	47.361710
23.768980	22.160000	161.274640	-75.753600	0.872406
39.000000	5.000000	174.469000	37.364900	75.247301
1.366345	1.038415	0.050516	0.993950	82.853865
0.996333	0.003667	182.940650	159.135560	47.350749
23.805090	22.160000	160.780650	-75.804292	0.797070
39.000000	10.000000	177.446000	37.347900	75.240200
1.323504	1.038421	0.049326	0.994547	79.432690
0.996828	0.003172	182.456090	158.613060	47.340378
23.843026	22.160000	160.296090	-75.858640	0.707559
39.000000	15.000000	180.146000	37.330000	75.232300
1.276735	1.038427	0.047982	0.995222	75.206291
0.997365	0.002635	181.962580	158.080230	47.330672
23.882353	22.160000	159.802580	-75.916019	0.609138
39.000000	20.000000	182.607000	37.311900	75.224001
1.226674	1.038433	0.046534	0.995949	70.129010
0.997914	0.002086	181.422810	157.500600	47.321660
23.922210	22.160000	159.262810	-75.975752	0.507590
39.000000	25.000000	184.789000	37.292900	75.215001
1.172513	1.038438	0.044931	0.996753	63.694429
0.998479	0.001521	180.853310	156.889940	47.313311
23.963367	22.160000	158.693310	-76.038689	0.399264
39.000000	30.000000	186.743000	37.274100	75.205901
1.115163	1.038442	0.043251	0.997596	55.671085
0.999014	0.000986	180.193390	156.188890	47.305701
24.004498	22.160000	158.033380	-76.103828	0.290659
39.000000	35.000000	188.535000	37.256501	75.198000
1.054732	1.038447	0.041574	0.998436	45.630520
0.999473	0.000527	179.333560	155.289870	47.298763
24.043686	22.160000	157.173560	-76.171210	0.186880
39.000000	40.000000	190.117000	37.239200	75.190601
0.990660	1.038450	0.039841	0.999304	30.962498
0.999841	0.000159	178.304140	154.221920	47.292475
24.082212	22.160000	156.144140	-76.241401	0.082345

39.000000	45.000000	191.465000	37.221800	75.183400
0.922642	1.038454	0.038026	1.000000	0.000000
1.000000	0.000000	177.100390	152.979760	47.286837
24.120636	22.160000	154.940390	-76.314698	-0.025092
39.000000	50.000000	192.591000	37.204400	75.177201
0.849864	1.038457	0.036149	1.000000	0.000000
1.000000	0.000000	175.625570	151.467430	47.281760
24.158136	22.160000	153.465570	-76.392091	-0.134765
39.000000	55.000000	193.520000	37.187800	75.171101
0.774616	1.038459	0.034266	1.000000	0.000000
1.000000	0.000000	173.897670	149.702670	47.277463
24.195000	22.160000	151.737670	-76.470906	-0.244218
40.000000	0.000000	194.293000	37.172700	75.164900
0.698407	1.038461	0.032436	1.000000	0.000000
1.000000	0.000000	171.894850	147.663930	47.274027
24.230924	22.160000	149.734850	-76.549497	-0.351002
40.000000	5.000000	194.800000	37.156701	75.158500
0.617616	1.038462	0.030505	1.000000	0.000000
1.000000	0.000000	169.561940	145.294260	47.271170
24.267677	22.160000	147.401940	-76.631910	-0.463902
40.000000	10.000000	194.895000	37.137500	75.149801
0.530867	1.038463	0.028288	1.000000	0.000000
1.000000	0.000000	166.949810	142.640970	47.268948
24.308848	22.160000	144.789810	-76.719338	-0.590465
40.000000	15.000000	194.711000	37.117700	75.139700
0.441227	1.038464	0.025992	1.000000	0.000000
1.000000	0.000000	163.877330	139.525550	47.267544
24.351774	22.160000	141.717330	-76.808460	-0.720346
40.000000	20.000000	194.382000	37.099300	75.130801
0.348949	1.038464	0.023837	1.000000	0.000000
1.000000	0.000000	159.990000	135.597390	47.266815
24.392609	22.160000	137.830000	-76.899374	-0.847106
40.000000	25.000000	193.867000	37.081600	75.123201
0.252669	1.038463	0.021825	1.000000	0.000000
1.000000	0.000000	155.054140	130.622390	47.266689
24.431748	22.160000	132.894140	-76.993565	-0.973869
40.000000	30.000000	193.145000	37.064200	75.116100
0.152808	1.038463	0.019985	1.000000	0.000000
1.000000	0.000000	148.907640	124.437420	47.267207
24.470223	22.160000	126.747640	-77.090503	-1.101849

40.000000	35.000000	192.191000	37.046700	75.108601
0.049861	1.038461	0.018355	1.000000	0.000000
1.000000	0.000000	141.379330	116.870170	47.268433
24.509159	22.160000	119.219330	-77.189542	-1.231824
40.000000	40.000000	191.004000	37.029200	75.101100
-0.056638	1.038459	0.017068	1.000000	0.000000
1.000000	0.000000	132.245980	107.697860	47.270354
24.548112	22.160000	110.085980	-77.291194	-1.363732
40.000000	45.000000	189.611000	37.011900	75.093900
-0.166509	1.038457	0.016286	1.000000	0.000000
1.000000	0.000000	121.617520	97.030863	47.272910
24.586658	22.160000	99.457522	-77.395375	-1.496896
40.000000	50.000000	187.989000	36.994700	75.086401
-0.279370	1.038455	0.016105	1.000000	0.000000
1.000000	0.000000	110.024410	85.398980	47.276205
24.625429	22.160000	87.864409	-77.501519	-1.631433
40.000000	55.000000	186.116000	36.977401	75.078401
-0.395455	1.038451	0.016585	1.000000	0.000000
1.000000	0.000000	98.270262	73.605507	47.280273
24.664755	22.160000	76.110261	-77.609791	-1.767733
41.000000	0.000000	184.001000	36.959900	75.070401
-0.515385	1.038448	0.017756	1.000000	0.000000
1.000000	0.000000	87.258507	62.554267	47.285013
24.704240	22.160000	65.098507	-77.720994	-1.906030
41.000000	5.000000	181.667000	36.942400	75.062701
-0.639038	1.038444	0.019565	1.000000	0.000000
1.000000	0.000000	77.692797	52.949339	47.290375
24.743458	22.160000	55.532797	-77.835086	-2.045803
41.000000	10.000000	179.113000	36.924900	75.055401
-0.766560	1.038439	0.021907	1.000000	0.000000
1.000000	0.000000	69.764249	44.981931	47.296351
24.782318	22.160000	47.604249	-77.952232	-2.187127
41.000000	15.000000	176.319000	36.907200	75.048100
-0.897881	1.038434	0.024670	1.000000	0.000000
1.000000	0.000000	63.287695	38.466360	47.302991
24.821336	22.160000	41.127696	-78.072260	-2.330079
41.000000	20.000000	173.295000	36.889400	75.041001
-1.033025	1.038429	0.027777	1.000000	0.000000
1.000000	0.000000	58.055592	33.195336	47.310270
24.860255	22.160000	35.895592	-78.195241	-2.474434

41.000000	25.000000	170.068000	36.872001	75.034001
-1.171005	1.038423	0.031143	1.000000	0.000000
1.000000	0.000000	53.868776	28.969965	47.318244
24.898811	22.160000	31.708776	-78.320099	-2.618987
41.000000	30.000000	166.666000	36.855200	75.027101
-1.311215	1.038417	0.034705	1.000000	0.000000
1.000000	0.000000	50.514598	25.577741	47.326880
24.936858	22.160000	28.354598	-78.446270	-2.763092
41.000000	35.000000	162.973000	36.837800	75.019401
-1.455233	1.038410	0.038465	0.999972	6.247319
0.999999	0.000001	47.635710	22.659611	47.336309
24.976099	22.160000	25.475711	-78.575074	-2.908385
41.000000	40.000000	158.961000	36.819500	75.010901
-1.603737	1.038402	0.042431	0.997986	51.359955
0.999237	0.000763	45.114413	20.097661	47.346539
25.016752	22.160000	22.954413	-78.707162	-3.054980
41.000000	45.000000	154.720000	36.801200	75.002401
-1.755652	1.038395	0.046560	0.995917	70.393264
0.997890	0.002110	42.991663	17.934242	47.357449
25.057421	22.160000	20.831663	-78.841696	-3.201425
41.000000	50.000000	150.229000	36.782801	74.993800
-1.911238	1.038386	0.050848	0.993769	83.854437
0.996179	0.003821	41.175330	16.077056	47.369085
25.09827 4	22.160000	19.015330	-78.978859	-3.347661
41.000000	55.000000	145.544000	36.764601	74.985400
-2.069787	1.038378	0.055261	0.991558	94.285772
0.994201	0.005799	39.640479	14.501668	47.381324
25.138811	22.160000	17.480479	-79.118129	-3.492879
42.000000	0.000000	140.739000	36.747100	74.979001
-2.232172	1.038369	0.059798	0.989285	102.775660
0.992006	0.007994	38.431188	13.254198	47.393889
25.176989	22.160000	16.271187	-79.260940	-3.638727
42.000000	5.000000	135.764000	36.730000	74.972700
-2.396831	1.038359	0.064422	0.986969	109.849590
0.989643	0.010357	37.399934	12.185135	47.407045
25.214800	22.160000	15.239934	-79.405186	-3.782965
42.000000	10.000000	130.465000	36.712200	74.965000
-2.565005	1.038349	0.069184	0.984582	115.942800
0.987109	0.012891	36.413289	11.158848	47.421126
25.254441	22.160000	14.253290	-79.551487	-3.924803

42.000000	15.000000	124.841000	36.693900	74.956201
-2.736931	1.038339	0.074091	0.982124	121.275280
0.984416	0.015584	35.484506	10.189016	47.436152
25.295491	22.160000	13.324506	-79.700072	-4.063576
42.000000	20.000000	119.004000	36.675700	74.947401
-2.911872	1.038328	0.079102	0.979613	125.964630
0.981596	0.018404	34.665433	9.328948	47.451828
25.336484	22.160000	12.505433	-79.850713	-4.198901
42.000000	25.000000	112.371000	36.655900	74.938601
-3.100062	1.038315	0.084525	0.976895	130.365840
0.978482	0.021518	33.866133	8.487467	47.469445
25.378666	22.160000	11.706133	-80.011862	-4.336038
42.000000	30.000000	106.752000	36.639600	74.931600
-3.272281	1.038304	0.089453	0.974425	133.881950
0.975606	0.024394	33.345047	7.928428	47.484767
25.416619	22.160000	11.185047	-80.160323	-4.459052
42.000000	35.000000	100.206000	36.621001	74.923400
-3.458677	1.038292	0.094837	0.971728	137.298010
0.972424	0.027576	32.760721	7.303327	47.502362
25.457394	22.160000	10.600721	-80.319615	-4.579857
42.000000	40.000000	93.346000	36.602100	74.914601
-3.649097	1.038279	0.100360	0.968959	140.424510
0.969122	0.030878	32.210327	6.711361	47.520863
25.498966	22.160000	10.050327	-80.481532	-4.690426
42.000000	45.000000	86.279001	36.583400	74.905801
-3.842295	1.038266	0.105975	0.966145	143.278020
0.965733	0.034267	31.718442	6.178033	47.540017
25.540409	22.160000	9.558442	-80.645242	-4.787741
42.000000	50.000000	79.148000	36.565500	74.897300
-4.036012	1.038252	0.111604	0.963324	145.864730
0.962309	0.037691	31.299593	5.718591	47.559519
25.581002	22.160000	9.139593	-80.808952	-4.867100
42.000000	55.000000	71.913000	36.547800	74.889000
-4.231224	1.038238	0.117281	0.960478	148.239360
0.958832	0.041168	30.928939	5.307663	47.579349
25.621276	22.160000	8.768939	-80.973637	-4.918243
43.000000	0.000000	64.257000	36.529400	74.879900
-4.432083	1.038223	0.123152	0.957536	150.484790
0.955216	0.044784	30.557944	4.895116	47.600316
25.662828	22.160000	8.397944	-81.142191	-4.905671

43.000000	5.000000	56.266000	36.510500	74.871001
-4.638457	1.038208	0.129195	0.954506	152.605620
0.951475	0.048525	30.212757	4.508179	47.622113
25.704579	22.160000	8.052758	-81.315004	
43.000000	10.000000	48.244000	36.491600	74.864201
-4.847926	1.038193	0.135304	0.951444	154.580590
0.947676	0.052324	29.938964	4.194579	47.643777
25.744386	22.160000	7.778964	-81.491216	
43.000000	15.000000	40.095000	36.473300	74.856501
-5.057363	1.038177	0.141429	0.948374	156.414070
0.943852	0.056147	29.682365	3.897758	47.666043
25.784607	22.160000	7.522365	-81.666376	

*37.	10.0	42095.	37.7693	75.4297
37.	15.0	50452.	37 .7508	75.4208
37.	20.0	58591.	37 .7334	75.4124
37.	25.0	66446.	37.7146	75.4042
37.	30.0	74133.	37 .6980	75.3969
37.	35.0	81562.	37.6814	75.3892
37.	40.0	88662.	37.6620	75.3798
37.	45.0	95534.	37.6435	75.3687
37.	50.0	102272.	37.6262	75.3649
37.	55.0	108694.	37.6071	75.3585
38.	05.0	120920.	37.5738	75.3401
38.	10.0	126706.	37.5569	75.3330
38.	15.0	132214.	37.5394	75.3254
38.	20.0	137492.	37.5219	75.3178
38.	25.0	142503.	37.5035	75.3095
38.	30.0	147288.	37.4859	75.3012
38.	35.0	151831.	37.4682	75.2930
38.	40.0	156116.	37.4493	75.2841
38.	45.0	160182.	37.4308	75.2754
38.	50.0	164051.	37.4131	75.2676
38.	55.0	167718.	37.3962	75.2602
39.	00.0	171200.	37.3805	75.2535
39.	05.0	174469.	37.3649	75.2473
39.	10.0	177446.	37.3479	75.2402
39.	15.0	180146.	37.3300	75.2323
39.	20.0	182607.	37.3119	75.2240

39.	25.0	184789.	37.2929	75.2150
39.	30.0	186743.	37.2741	75.2059
39.	35.0	188535.	37.2565	75.1980
39.	40.0	190117.	37.2392	75.1906
39.	45.0	191465.	37.2218	75.1834
39.	50.0	192591.	37.2044	75.1772
39.	55.0	193520.	37.1878	75.1711
40.	00.0	194293.	37.1727	75.1649
40.	05.0	194800.	37.1567	75.1585
40.	10.0	194895.	37.1375	75.1498
40.	15.0	194711.	37.1177	75.1397
40.	20.0	194382.	37.0993	75.1308
40.	25.0	193867.	37.0816	75.1232
40.	30.0	193145.	37.0642	75.1161
40.	35.0	192191.	37.0467	75.1086
40.	40.0	191004.	37.0292	75.1011
40.	45.0	189611.	37.0119	75.0939
40.	50.0	187989.	36.9947	75.0864
40.	55.0	186116.	36.9774	75.0784
41.	00.0	184001.	36.9599	75.0704
41.	05.0	181667.	36.9424	75.0627
41.	10.0	179113.	36.9249	75.0554
41.	15.0	176319.	36.9072	75.0481
41.	20.0	173295.	36.8894	75.0410
41.	25.0	170068.	36.8720	75.0340
41.	30.0	166666.	36.8552	75.0271
41.	35.0	162973.	36.8378	75.0194
41.	40.0	158961.	36.8195	75.0109
41.	45.0	154720.	36.8012	75.0024
41.	50.0	150229.	36.7828	74.9938
41.	55.0	145544.	36.7646	74.9854
42.	00.0	140739.	36.7471	74.9790
42.	05.0	135764.	36.7300	74.9727
42.	10.0	130465.	36.7122	74.9650
42.	15.0	124841.	36.6939	74.9562
42.	20.0	119004.	36.6757	74.9474
42.	25.0	112371.	36.6559	74.9386
42.	30.0	106752.	36.6396	74.9316
42.	35.0	100206.	36.6210	74.9234
42.4	40.0	93346.	36.6021	74.9146
42.	45.0	86279.	36.5834	74.9058
42.	50.0	79148.	36.5655	74.8973
42.	55.0	71913.	36.5478	74.8890
43.	00.0	64257.	36.5294	74.8799
43.	05.0	56266.	36.5105	74.8710
43.	10.0	4824436.4916		74.8642
43.	15.0	40095.	36.4733	74.8565

APPENDIX B

SOLAR ASPECT DATA REDUCTION

In previous rocket flights, solar aspect data reduction was effectively carried out by scaling the time intervals "t", from a chart record run at 10 IPS. Experience has shown that slightly less than optimum results are obtained when using this method of reduction. The following system has been devised and successfully used, as a more accurate and efficient method of obtaining these times. The system is a digital counting device which generates two pulses, a start and a stop command. All magnetic tape flight records contain a 100 KHz sinusoidal reference frequency. The 100 KHz signal, when controlled by start and stop pulses, is used to measure "t" with little or no effect from tape speed variation. Accuracy is improved by eliminating the tedious job of scaling from a 10 IPS paper record.

The following describes the system and its uses.

To measure time intervals between the first and last solar aspect pulses for a desired number of revolutions, the system monitors the 100 KHz signal placed on the tape during a flight recording. For the case being discussed an H.P. Model 5244L Digital Counter was modified slightly, to allow external control of start and stop counting commands. Commercial counters are available with this feature built in. The modification allowed us to sample the 100 KHz signal during the time interval between start and stop commands. The Digital Counter is then connected to a high speed digital printer, H.P. Model 5050A, capable of printing up to 20 lines of 6 characters per second. The counter is then placed in the manual position. In this mode it accumulates the number of cycles the 100 KHz goes through for the interval between start and stop. Since most Nike-Apache payloads have a spin rate of under 10 rps the system is capable of printing real time "t" values.

Following the stop command, the counter internally generates print and reset commands. The print command is sent to the high speed printer, the reset command clears the digital counter for the next data point. Figure B-1 is a block diagram of the system.

The start-stop commands are derived from the solar aspect pulses. The circuitry consists of:

(1) a Shmidt trigger for pulse shaping. This circuit insures good sharp rise times for all pulses; it also can be adjusted for varying thresholds, depending on the quality of the signal.

(2) The pulses are then inserted into a two-stage ripple counter, which consists of two J-K flip flops. The flip flops are triggered on

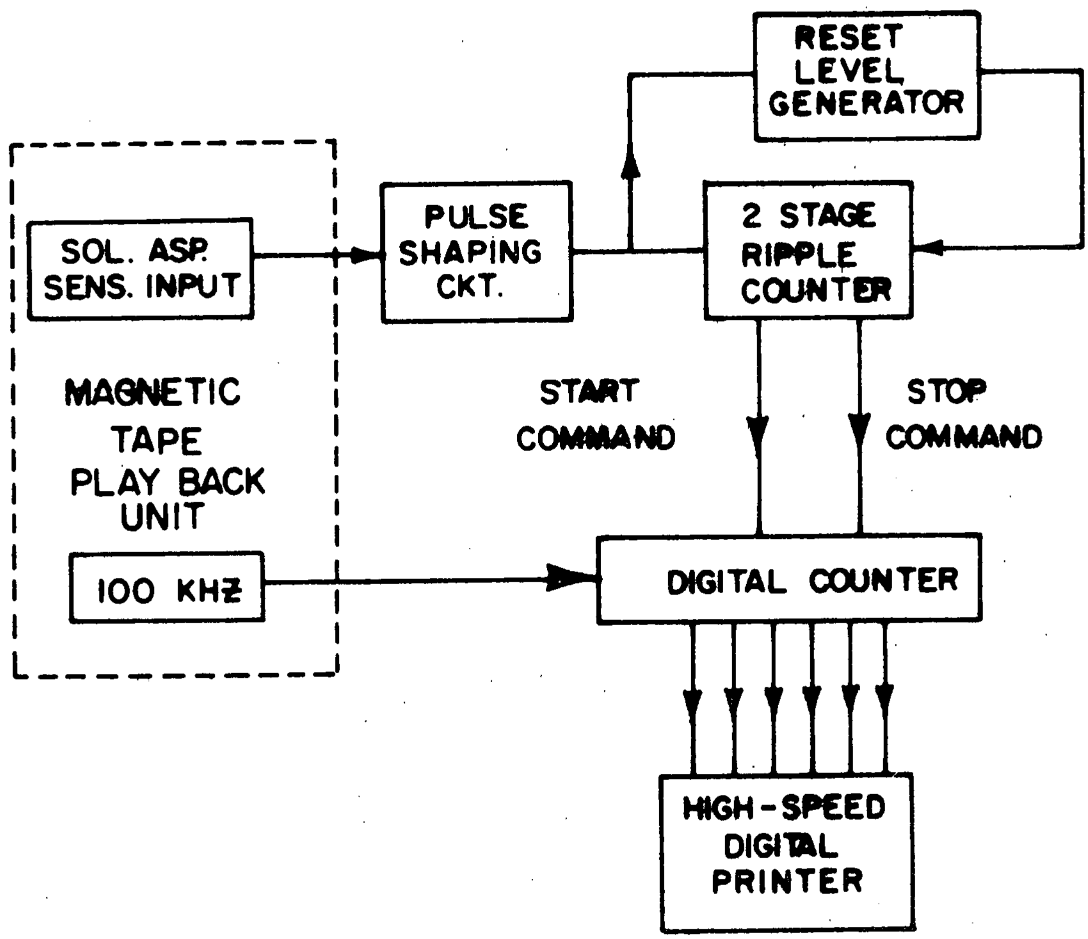

Figure B-1. Solar aspect angle data reduction scheme.

the rising edges of the Shmidt output. A "reset" pulse generator is also triggered on the first pulse arriving at the input. The function of this reset generator is to insure that the system maintains sync with the solar aspect data. The reset level time is determined by the spin rate of the vehicle in question. The reset pulse width is selected to be one-half the time required for one revolution of the vehicle. The reset generator clears the ripple counter to its "0,0" state.

Since the maximum time between the first and last pulse edge is about one-third the vehicle spin rate and the spin is essentially constant through the time interval of interest, a reset signal generated at one-half the spin rate insures synchronism between the magnetic tape data and the digital system. If the two should become out of sync, the system would recover in 1 rps, by virtue of the reset pulse. The start-stop pulses are generated by gating the "1,1" state of the ripple counter for the start and the "0" state of the second flip flop for the stop. Resetting is accomplished by using integrated circuit flip flops with "clear" inputs accessible for asynchronous resetting.

To eliminate ambiguity with respect to positive and negative aspect angles, the solar aspect sensor is designed to generate a 3 pulse signal for positive cycles ($0^\circ \rightarrow +70^\circ$) and 2 pulses for negative angles ($0^\circ \rightarrow -70^\circ$).

Each number on the printer tape corresponds to the number of 100 KHz cycles between start and stop intervals. The exact time of each reading is obtained by running a chart record of the solar pulses, along with the start and stop pulses. In this manner each "stop" and therefore "print" command can be accounted for at a particular time. If noise should cause a false print, one can immediately determine its location by inspecting the printed output for an irregular number. Since the data are generally slowly varying quantities, irregularities are quickly ascertained.

In addition to the chart record, a 100 KHz signal interrupt switch is used to mark 10 second intervals on the printer output. The result of the 100 KHz interrupt is a blank space on the printer output, that is, when the 100 KHz is interrupted, the printer suppresses the zeros and a blank is recorded. We therefore have 10 second "blank space" markers on the printer output for time reference.

This system has been successfully utilized for 11 rocket flights to date. This includes the vehicles flown during the 1970 eclipse operation. The solar aspect data from these flights show that under the worst conditions, an accuracy of 0.3 degrees aspect angle can be reached.

INPUT FORMAT

REV NO.	T1	T2	REV NO.	T1	T2	REV NO.	T1	T2	REV NO.	T1	T2
*95	21.10	119.	96	21.03	119.	97	20.85	119.	98	20.68	119.
99	20.59	119.	100	20.34	119.	101	20.22	119.	102	20.01	119.
103	19.84	119.	104	19.54	119.	105	19.38	119.	106	19.20	119.
107	19.01	119.	108	18.84	119.	109	18.61	119.	110	18.39	119.
111	18.18	119.	112	17.82	119.	160	18.35	121.	161	18.61	121.
162	18.94	121.	163	19.21	121.	164	19.50	121.	165	19.80	122.
166	20.14	122.	167	20.40	122.	168	20.72	122.	169	20.99	122.
170	21.41	123.	171	21.65	123.	172	21.96	123.	173	22.22	123.
174	22.60	123.	175	22.86	124.	176	23.15	124.	177	23.39	124.
178	23.72	124.	179	23.97	125.	180	24.35	125.	181	24.64	125.
182	24.91	125.	183	25.17	125.	184	25.41	126.	185	25.69	125.
186	25.96	125.	187	26.23	127.	188	26.52	127.	189	26.76	127.
190	27.01	128.	191	27.30	128.	192	27.51	128.	193	27.80	128.
194	28.09	129.	195	28.32	129.	196	28.54	129.	197	28.77	129.
198	28.96	130.	199	29.24	130.	200	29.48	130.	201	29.61	130.
202	29.93	130.	203	30.03	131.	204	30.32	131.	205	30.58	131.
206	30.76	132.	207	31.03	132.	208	31.21	133.	209	31.46	134.
210	31.67	134.	211	31.90	135.	212	32.08	135.	213	32.26	136.
214	32.53	136.	215	32.70	137.	216	32.84	137.	217	33.12	137.
218	33.38	138.	219	33.51	138.	220	33.74	138.	221	33.85	138.
222	34.08	139.	223	34.29	140.	224	34.50	140.	225	34.66	141.
226	34.87	142.	227	35.15	142.	228	35.28	143.	229	35.45	144.
230	35.58	144.	231	35.79	145.	232	35.99	145.	234	36.39	147.
235	36.53	148.	236	36.65	148.	237	36.91	149.	238	37.08	15.
239	37.24	150.	240	37.43	151.	241	37.58	152.	242	37.67	153.

OUTPUT FORMAT

REV NO.	ASPECT ANGLE	REV NO.	ASPECT ANGLE	REV NO.	ASPECT ANGLE	REV NO.	ASPECT ANGLE	REV NO.	ASPECT ANGLE
95	56.20	96	56.29	97	56.52	98	56.74	99	56.85
100	57.16	101	57.31	102	57.56	103	57.76	104	58.11
105	58.30	106	58.50	107	58.71	108	58.90	109	59.15
110	59.38	111	59.60	112	59.97	160	59.74	161	59.48
162	59.13	163	58.84	164	58.53	165	58.37	166	57.99
167	57.69	168	57.32	169	57.00	170	56.69	171	56.40
172	56.00	173	55.67	174	55.16	175	55.06	176	54.66
177	54.33	178	53.86	179	53.77	180	53.22	181	52.78
182	52.37	183	51.96	184	51.90	185	51.11	186	50.66
187	50.90	188	50.42	189	50.01	190	49.94	191	49.44
192	49.07	193	48.54	194	48.41	195	47.99	196	47.58
197	47.14	198	47.20	199	46.66	200	46.19	201	45.93
202	45.28	203	45.54	204	44.95	205	44.40	206	44.52
207	43.94	208	44.06	209	44.03	210	43.58	211	43.60
212	43.21	213	43.34	214	42.76	215	42.91	216	42.61
217	41.99	218	41.95	219	41.67	220	41.15	221	40.90
222	40.94	223	41.02	224	40.54	225	40.74	226	40.82
227	40.19	228	40.45	229	40.62	230	40.34	231	40.42
232	39.97	234	40.19	235	40.42	236	40.16	237	40.13
238	-53.24	239	39.96	240	40.08	241	40.29	242	40.61

INPUT FORMAT

REV NO.	T1	T2	REV NO.	T1	T2	REV NO.	T1	T2	REV NO.	T1	T2
*243	37.93	153.	244	38.02	154.	245	38.16	155.	246	38.39	156.
247	38.46	157.	248	38.69	158.	249	38.84	159.	250	38.94	160.
251	39.04	161.	252	39.25	162.	253	39.42	163.	254	39.46	164.
255	39.69	1655.									
255	39.69	165.	256	39.77	166.	257	39.92	167.	258	39.96	168.
259	40.10	169.	260	40.08	170.	261	40.27	172.	262	40.24	172.
263	40.40	173.	264	40.49	174.	265	40.64	175.	266	40.61	176.
267	40.71	178.	268	40.70	179.	269	40.77	180.	270	40.73	182.
271	40.81	183.	272	40.87	185.	273	40.87	186.	274	40.92	188.
275	40.85	190.	276	40.97	191.	277	40.89	193.	278	40.92	195.
279	40.86	197.	280	40.80	199.	281	40.73	201.	282	40.73	203.
283	40.57	205.	284	40.41	207	285	40.31	209	286	40.13	211.
8											
287	39.93	213.	288	39.74	216.	289	39.46	219.	291	38.97	224.
292	38.54	227.	293	38.17	230.	294	37.77	233.	295	37.38	238.
296	37.02	241.	297	36.53	244.	298	36.11	247.	299	35.71	251.
300	35.16	254.	306	32.67	273.	307	32.60	276.	308	32.59	278.
309	32.71	281.	310	32.93	285.	311	33.38	290.	312	33.96	294.
313	34.75	298.	314	35.64	303	315					
313	34.75	298.	314	35.64	303.	315	36.80	307.	316	38.22	312
313	34.75	298.	314	35.64	303.	315	36.80	307.	317	38.22	312.
318	41.46	322.	319	43.42	327.	320	45.71	331.	321	48.14	334.
322	50.59	337.	323	53.11	341.	324	54.23	343.	325	55.90	345.
327	59.84	347.	328	61.09	347.	329	63.32	347.	330	64.71	348.
331	65.69	348	332	67.93	348.	333	69.17	348.	334	69.96	348.
335	72.03	349.	336	73.01	349.	337	73.74	349.	338	75.69	349.
339	76.51	349.	340	777.							
339	76.51	349.	340	77.12	349.	341	78.84	349.	342	79.45	349.
343	79.99	350.	344	81.59	350.	345	81.95	350.	346	82.49	350.
347	83.97	350.	348	84.01	350.	349	84.47	350.	350	85.86	350.

OUTPUT FORMAT

REV NO.	ASPECT ANGLE	REV NO.	ASPECT ANGLE	REV NO.	ASPECT ANGLE	REV NO.	ASPECT ANGLE	REV NO.	ASPECT ANGLE
243	40.07	244	40.40	245	40.62	246	40.65	247	41.01
248	41.03	249	41.22	250	41.50	251	41.77	252	41.83
253	41.97	254	42.34	255	42.36	256	42.64	257	42.80
258	43.15	259	43.32	260	43.75	261	44.21	262	44.26
263	44.38	264	44.61	265	44.74	266	45.14	267	45.68
268	46.03	269	46.26	270	46.95	271	47.14	272	47.66
273	47.94	274	48.43	275	49.05	276	49.16	277	49.76
278	50.20	279	50.72	280	51.22	281	51.70	282	52.10
283	52.63	284	53.14	285	53.57	286	54.05	287	54.53
288	55.12	289	55.74	291	56.71	292	57.33	293	57.87
294	58.40	295	59.06	296	59.50	297	59.97	298	60.39
299	60.84	300	61.26	306	63.12	307	63.27	308	63.34
309	63.42	310	63.49	311	63.53	312	63.50	313	63.40
314	63.31	315	63.11	317	62.86	318	62.26	319	61.85
320	61.29	321	60.63	322	59.93	323	59.23	324	58.93
325	58.41	327	56.94	328	56.39	329	55.37	330	54.79
331	54.30	332	53.14	333	52.47	334	52.02	335	50.93
336	50.34	337	49.88	338	48.62	339	48.06	340	47.64
341	46.41	342	45.96	343	45.73	344	44.49	345	44.21
346	43.77	347	42.54	348	42.51	349	42.12	350	40.90

INPUT FORMAT

	REV NO.	T1	T2	REV NO.	T1	T2	REV NO.	T1	T2	REV NO.	T1	T2
00099	62											
00100	351	85.82	350.	352	86.31	350.	353	87.46	350.	354	87.21	350.
00110	355	87.69	350.	356	88.54	350.	357	88.17	350.	358	88.78	350.
00120	359	89.27	350.	360	88.86	350.	361	89.46	350.	362	89.75	350.
00130	363	89.14	350.	364	89.77	350.	365	89.75	350.	366	89.18	350.
00160	367	89.76	350.	368	89.59	350.	369	88.92	350.	370	89.35	350.
00170	371	88.87	350.	372	88.24	350.	373	88.60	350.	374	87.79	350.
00180	375	87.24	350.	376	87.50	350.	377	86.32	350.	378	85.89	350.
00190	379	85.79	350.	380	84.59	349.	381	84.10	349.	382	83.76	349.
00200	383	69.75	349.	384	81.92	349.	385	81.25	349.	386	79.89	349.
00210	387	79.28	349.	388	78.30	349.	389	76.82	349.	390	76.10	349.
00230	391	74.94	349.	392	73.32	349.	393	72.48	349.	394	71.02	349.
00240	395	69.23	349.	396	68.18	349.	397	66.23	349.	398	64.57	349.
00250	399	63.13	349.	400	61.16	349.	401	59.21	349.	402	57.62	349.
00260	403	55.36	349.	404	53.24	349.	405	51.44	349.	406	49.08	349.
00270	407	46.92	349.	408	45.11	349.	409	42.88	349.	410	40.98	349.
00280	238	37.08	150.									

OUTPUT FORMAT

REV NO.	ASPECT ANGLE	REV NO.	ASPECT ANGLE	REV NO.	ASPECT ANGLE	REV NO.	ASPECT ANGLE	REV NO.	ASPECT ANGLE
351	40.93	352	40.49	353	39.43	354	39.66	355	39.21
356	38.40	357	38.75	358	38.16	359	37.68	360	38.08
361	37.49	362	37.20	363	37.81	364	37.18	365	37.20
366	37.77	367	37.19	368	37.36	369	38.02	370	37.60
371	38.07	372	38.69	373	38.34	374	39.12	375	39.63
376	39.39	377	40.48	378	40.87	379	40.96	380	41.80
381	42.23	382	42.52	383	52.25	384	44.04	385	44.58
386	45.63	387	46.09	388	46.80	389	47.85	390	48.34
391	49.11	392	50.15	393	50.66	394	51.53	395	52.54
396	53.11	397	54.13	398	54.95	399	55.63	400	56.51
401	57.35	402	57.99	403	58.86	404	59.63	405	60.25
406	61.02	407	61.68	408	62.21	409	62.83	410	63.33
238	40.30	0	70.00	0	0.00	0	0.00	0	0.00

INPUT FORMAT

REV NO.	T1	T2	REV NO.	T1	T2	REV NO.	T1	T2	REV NO.	T1	T2
64	35.42	180.	65	35.90	180.	66	35.27	180.	67	35.80	180.
68	35.16	180.	69	35.59	180.	70	35.18	180.	71	35.67	180.
72	36.14	180.	73	36.60	180.	74	36.06	180.	75	36.21	180.
76	36.81	180.	77	36.42	180.	78	36.78	180.	79	36.60	180.
82	37.56	180.	83	37.17	181.	84	37.00	181.	85	37.02	181.
86	37.18	181.	87	37.69	181.	88	38.34	181.	91	38.02	181.
92	38.26	181.	93	38.45	181.	94	37.90	181.	95	38.34	181.
96	38.79	181.	97	38.67	181.	98	38.85	181.	99	39.71	182.
100	39.50	182.	101	39.29	182.	102	39.35	182.	103	40.01	182.
104	39.98	182.	105	39.74	182.	106	39.99	183.	107	40.28	183.
108	40.36	183.	109	40.44	184.	110	40.83	184.	111	40.97	185.
112	41.43	185.	113	41.04	185.	114	41.50	186.	115	41.62	186.
116	41.84	186.	117	41.68	187.	118	41.72	187.	119	42.25	187.
120	42.47	188.	121	42.63	188.	122	43.08	189.	123	43.06	189.
124	43.57	190.	125	43.51	190.	126	44.12	191.	127	44.54	192.
128	44.52	193.	129	44.73	194.	130	45.12	195.	131	45.05	195.
132	45.26	196.	133	45.46	196.	134	45.84	197.	135	45.79	198.
136	46.13	199.	137	46.77	200.	138	46.75	200.	139	47.08	201.
140	47.22	202.	141	47.73	203.	142	47.96	204.	143	48.21	205.
144	48.66	206.	145	48.75	207.	146	49.01	108.	147	49.09	209.
148	50.12	210.	149	50.19	211.	150	51.22	212.	151	50.25	214.
152	50.67	215.	153	51.20	216.	154	51.73	217.	155	52.09	218.
156	52.40	220.	157	52.81	221.	158	52.76	222.	159	53.38	225.
160	55.21	227.	161	54.05	228.	162	54.25	229.	163	55.25	230.
164	55.39	232.	165	55.83	234.	166	56.40	236.	167	56.07	238.

OUTPUT FORMAT

REV NO.	ASPECT ANGLE	REV NO.	ASPECT ANGLE	REV NO.	ASPECT ANGLE	REV NO.	ASPECT ANGLE	REV NO.	ASPECT ANGLE
64	52.85	65	52.33	66	53.00	67	52.44	68	53.12
69	52.67	70	53.10	71	52.58	72	52.07	73	51.56
74	52.16	75	52.00	76	51.32	77	51.76	78	51.36
79	51.56	82	50.45	83	51.15	84	51.34	85	51.32
86	51.14	87	50.54	88	49.76	91	50.15	92	49.86
93	49.63	94	50.30	95	49.76	96	49.21	97	49.36
98	49.13	99	48.31	100	48.58	101	48.85	102	48.77
103	47.92	104	47.96	105	48.27	106	48.23	107	47.85
108	47.75	109	47.93	110	47.41	111	47.52	112	46.91
113	47.43	114	47.11	115	46.95	116	46.66	117	47.17
118	47.12	119	46.40	120	46.41	121	46.19	122	45.88
123	45.91	124	45.52	125	45.60	126	45.07	127	44.80
128	45.16	129	45.19	130	44.97	131	45.06	132	45.09
133	44.82	134	44.61	135	45.00	136	44.85	137	44.29
138	44.32	139	44.18	140	44.31	141	43.93	142	43.94
143	43.92	144	43.62	145	43.82	146	-49.53	147	44.00
148	42.91	149	43.15	150	42.04	151	44.02	152	43.78
153	43.39	154	42.99	155	42.83	156	43.05	157	42.83
158	43.21	159	43.33	160	41.55	161	43.38	162	43.43
163	42.45	164	42.89	165	42.94	166	42.82	167	43.80

INPUT FORMAT

REV NO.	T1	T2	REV NO.	T1	T2	REV NO.	T1	T2	REV NO.	T1	T2
168	57.09	240.	169	57.36	242.	170	57.72	244.	171	58.43	247.
172	58.84	249.	173	59.35	251.	174	59.88	253.	175	60.12	255.
176	60.64	257.	177	61.10	260.	178	61.98	263.	179	62.39	267.
180	63.02	269.	181	63.47	271.	183	64.37	276.	184	65.18	280.
185	65.46	284.	186	66.52	287.	187	66.91	290.	188	67.43	293.
189	68.58	297.	190	32.09	301.	191	69.83	304.	192	70.53	309.
193	71.26	313.	194	71.76	317.	195	72.63	321.	196	73.54	325.
197	74.43	329.	198	75.22	334.	199	75.73	339.	200	76.92	344.
201	78.11	350.	202	78.66	356.	203	79.71	362.	204	80.72	368.
205	81.51	375.	206	82.77	382.	207	83.85	389.	208	84.72	397.
209	86.32	405.	210	87.62	413.	211	88.15	420.	212	90.07	429.
213	91.29	438.	215	93.76	455.	216	95.40	466.	217	97.17	477.
218	98.89	488.	219	101.46	498.	220	102.70	506.	221	105.72	514.
222	108.16	520.	223	107.90	526.	224	106.77	531.	225	108.19	535.
226	106.06	536.	229	106.89	536.	230	106.91	536.	231	106.08	536.
232	107.05	536.	233	107.02	536.	234	107.69	536.	235	108.32	536.
236	108.75	537.	237	109.22	537.	238	108.80	537.	240	109.46	537.
241	110.88	537.	242	110.61	537.	243	112.68	537.	244	112.72	537.
245	113.12	537.	246	114.07	537.	247	114.48	537.	248	115.46	537.
249	115.33	537.	250	116.61	537.	251	116.31	537.	252	118.23	537.
253	118.30	537.	254	119.54	537.	256	121.07	537.	257	121.45	537.
260	122.72	537.	261	123.20	537.	262	124.00	537.	263	124.17	537.
264	124.83	537.	265	125.52	537.	266	125.72	537.	267	125.83	537.
268	126.08	537.	269	126.58	537.	270	127.06	537.	271	126.93	537.
272	126.90	537.	273	127.99	537.	274	127.46	537.	275	127.84	537.

OUTPUT FORMAT

REV NO.	ASPECT ANGLE	REV NO.	ASPECT ANGLE	REV NO.	ASPECT ANGLE	REV NO.	ASPECT ANGLE	REV NO.	ASPECT ANGLE
168	43.14	169	43.39	170	43.52	171	43.52	172	43.60
173	43.55	174	43.49	175	43.75	176	43.70	177	43.97
178	43.78	179	44.34	180	44.17	181	44.19	183	44.46
184	44.58	185	45.21	186	44.86	187	45.14	188	45.30
189	45.09	190	64.25	191	45.42	192	45.80	193	45.96
194	46.29	195	46.32	196	46.32	197	46.33	198	46.59
199	47.05	200	46.99	201	47.10	202	47.65	203	47.83
204	48.03	205	48.50	206	48.66	207	48.92	208	49.41
209	49.47	210	49.69	211	50.19	212	50.17	213	50.50
215	51.00	216	51.28	217	51.49	218	51.70	219	51.48
220	51.64	221	51.08	222	50.59	223	51.19	224	52.01
225	51.79	226	52.64	229	52.34	230	52.33	231	52.63
232	52.28	233	52.29	234	52.05	235	51.81	236	51.73
237	51.55	238	51.71	240	51.46	241	50.91	242	51.02
243	50.20	244	50.18	245	50.02	246	49.63	247	49.46
248	49.05	249	49.10	250	48.55	251	48.68	252	47.84
253	47.81	254	47.24	256	46.53	257	46.34	260	45.73
261	45.49	262	45.09	263	45.01	264	44.67	265	44.32
266	44.21	267	44.16	268	44.03	269	43.76	270	43.51
271	43.58	272	43.59	273	43.01	274	43.29	275	43.09

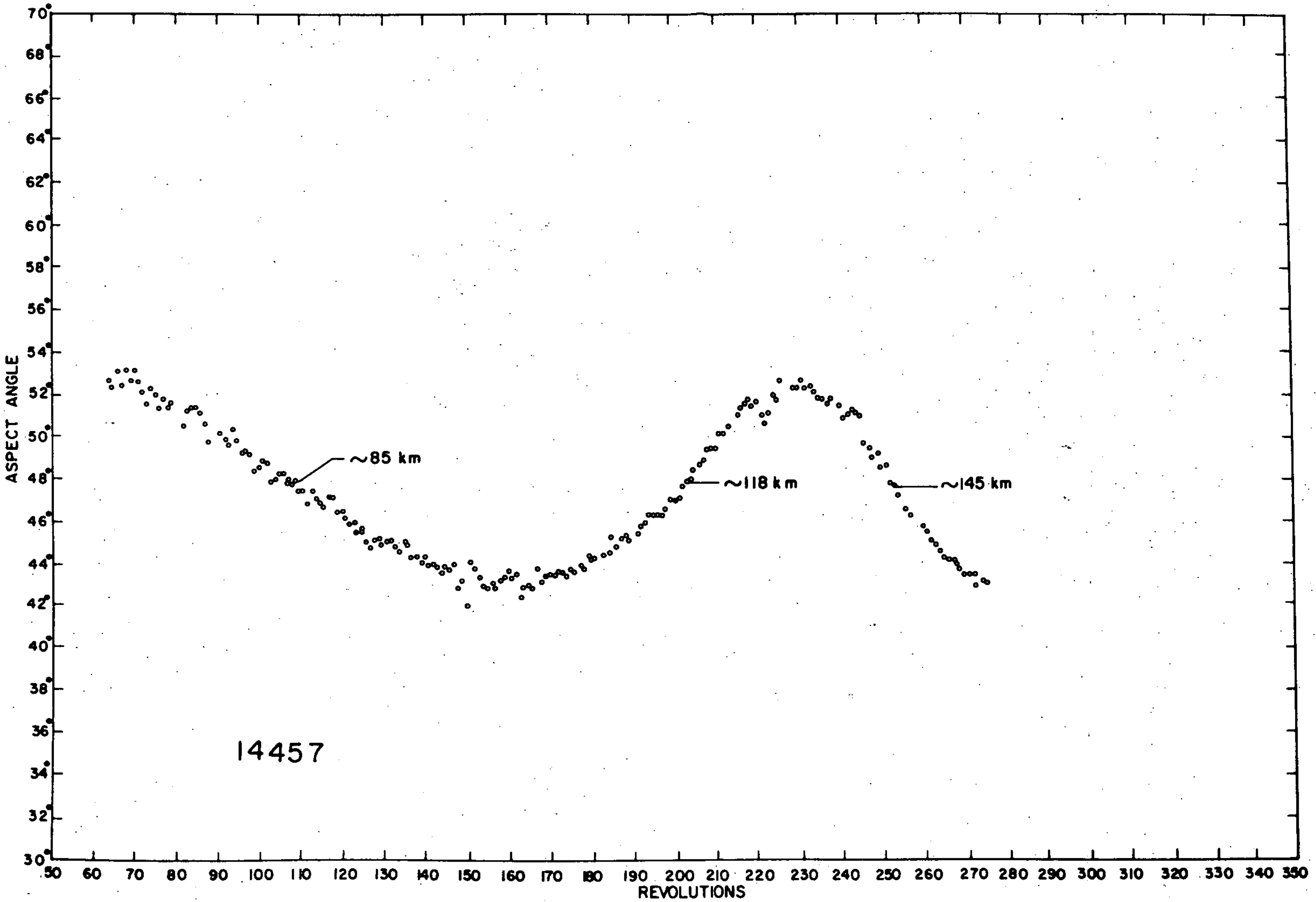
ASPECT ANGLE
70°
68°
66°
64°
62°
60°
58°
56°
54°
52°
50°
48°
46°
44°
42°
40°
38°
36°
34°
32°
30°
50 60 70 80 90 100 110 120 130 140 150 160 170 180 190 200 210 220 230 240 250 260 270 280 290 300 310 320 330 340 350
REVOLUTIONS
~85 km
~118 km
~145 km
14457

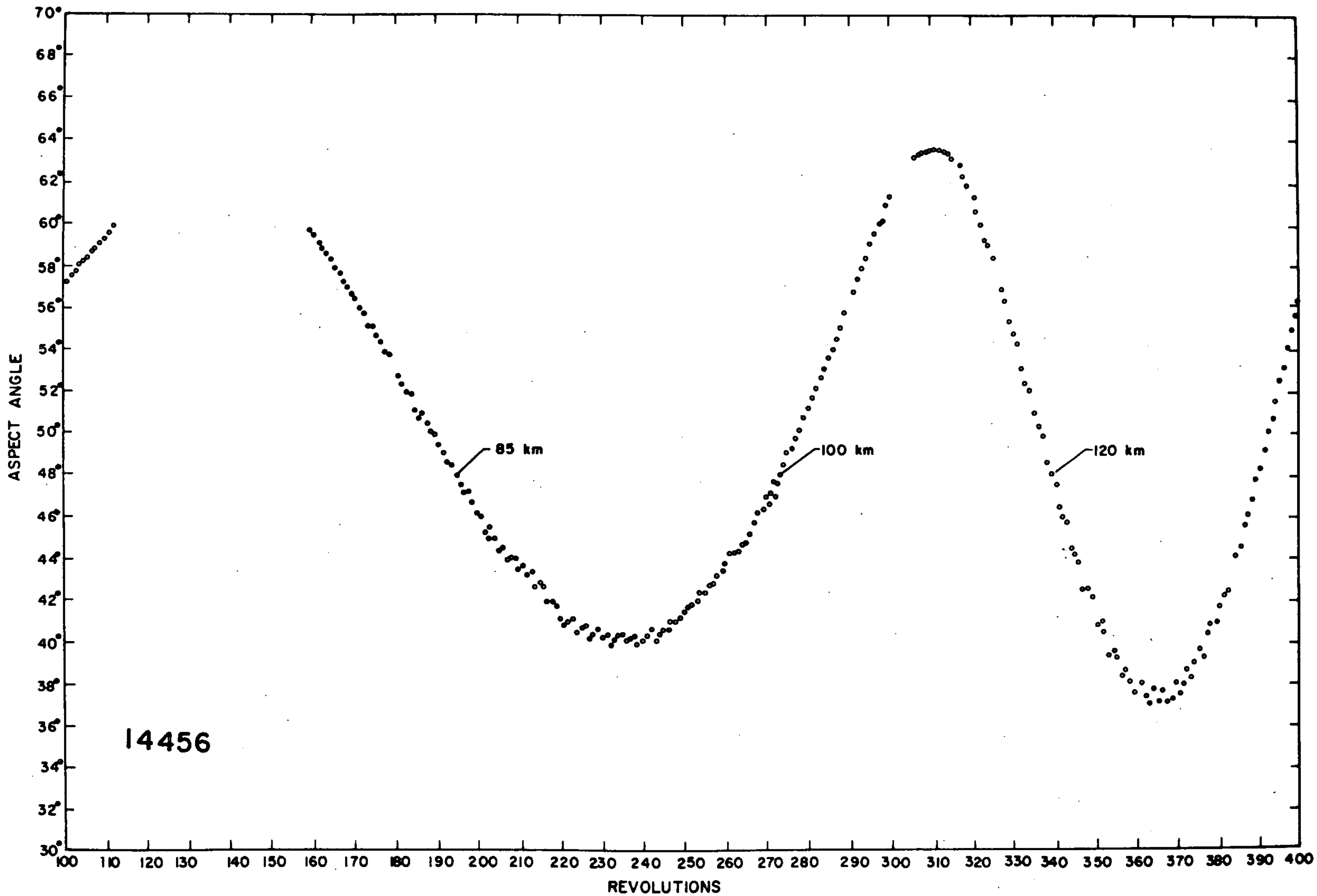
ASPECT ANGLE
70°
68°
66°
64°
62°
60°
58°
56°
54°
52°
50°
48°
46°
44°
42°
40°
38°
36°
34°
32°
30°
85 km
100 km
120 km
14456
100 110 120 130 140 150 160 170 180 190 200 210 220 230 240 250 260 270 280 290 300 310 320 330 340 350 360 370 380 390 400
REVOLUTIONS

APPENDIX C

SOLAR X-RAY ATMOSPHERIC ABSORPTION PROFILE PROGRAM

The computer program absorbifor generates atmospheric absorption profiles for X-rays between 1 and 100Å for altitudes between 80 and 129 km. A black-body solar flux distribution is combined with corresponding Geiger counter efficiencies and model atmospheric cross sections to produce the desired absorption characteristics.

The input data file required to execute the program consists of (a) the number of Feiger counter wavelength-efficiency pairs describing the efficiency curve, (b) the black-body temperature chosen, (c) the wavelength efficiency data points, and (d) the X-ray band of interest.

The computer program performs a numerical integration with 20 iterations and generates successive solutions for

$$\int_{\lambda_1}^{\lambda} \Sigma(\lambda) \left(\frac{dn}{d\lambda}\right) \text{Exp}\left[-(\sigma)\ n(z)\ n_T\ \sec(x)\right]$$

where x is the angle of incident radiation. For the 7 March eclipse, $x = 47.4^{\circ}$.

```
ABSORB.FOR
DO.100 I=80,120
ALT I
READ (1,10)NDATA
DIMENSION WVLNT(100),EFCNCY(100),ALTUD(50),P(50)
COMMON WVLNT,EFCNCY,NDATA,AT,ALT,P,G,GAM,CHI
READ (1,25)AT
FORMAT(E )
DO 50 I=1,NDATA
READ(1,20)WVLNT(I),EFCNCY(I)
WVLNT(I)=WVLNT(I)*1.E-08
CONTINUE
READ(1,30)K1,K2
PI=3.1415927
AC=2.99793E+10
AH=6.62517E+27
AKON=2.*PI*AC
ITER=20
AK1=K1
XA=AK1*1.E-08
AK2=K2
XB=AK2*1.E-08
ALT=1000.
CALLITRPZ(XA,XB,ITER,COUNTS)
CMAX=COUNTS*AKON
TYPE 90,CMAX
DO 100 I=80,129
ALT=I
CALL ITRPZ(XA,XB,ITER,COUNTS)
COUNTS=COUNTS*AKON
PERCNT=COUNTS/CMAX
TYPE 60,ALT,COUNTS,PERCNT
FORMAT(I )
FORMAT(2F )
FORMAT(2I )
FORMAT(1X,F5.1,2(1PE15.5))
FORMAT(1X,1PE15.5)
CONTINUE
END
SUBROUTINE ITRPZ(XA,XB,ITER,E)
COMMON CHI
HITER=ITER
DX=(XB-XA)/HITER
COUNTS=Y(XA)/2.
X=XA
DO 100 I=2,ITER
X=X+DX
COUNTS=COUNTS+Y(X)
CONTINUE
E=(COUNTS+Y(XB)/2.)*DX
RETURN
END
```

```
      SUBROUTINE XYFCN(XDATA,YDATA,NDATA,X,Y)
      DIMENSION XDATA(100),YDATA(100)
      IF(X-XDATA(1))120,105,110
      Y=YDATA(1)
      GO TO 145
      IF(X-XDATA(NDATA))130,115,120
      Y=YDATA(NDATA)
      GO TO 145
      TYPE 125,X
      FORMAT(1PE15.8)
      STOP
      DO 135 I=2,NDATA
      IF(X-XDATA(I))140,135,135
      CONTINUE
      IM=I-1
      Y=YDATA(IM)+(YDATA(I)-YDATA(IM))*(X-XDATA(IM))/
     1(XDATA(I)-XDATA(IM))
      RETURN
      END
      SUBROUTINE PRESUR(ALT,PRES)
      DIMENSION ALTUD(50),P(50)
      DATA ALTUD/80.,81.,82.,83.,84.,85.,86.,87.,88.,
     189.,90.,91.,92.,93.,94.,95.,96.,97.,98.,99.,100.,
     2101.,102.,103.,104.,105.,106.,107.,108.,109.,110.,
     3111.,112.,113.,114.,115.,116.,117.,118.,119.,120.,
     4121.,122.,123.,124.,125.,126.,127.,128.,129./
      DATA P/9.745,8.149,6.814,5.699,4.766,3.986,3.334,
     12.789,2.333,1.952,1.633,1.368,1.149,0.9673,0.8164,
     20.6907,0.5857,0.4978,0.4240,0.3619,.3095,.2655,.2285,
    3.1974,.1710,.1486,.1296,.1133,.0993,.08727,.0769,
     4.06802,.06049,.05404,.0485,.0437,.03952,.03587,.03267,
     5.02984,.02733,.02511,.02314,.02139,.01982,.01841,
     6.01714,.0160,.01496,.01401/
      DO 20 I=1,50
      IF(ALTUD(I)-ALT)20,40,50
      FORMAT(41HPRESSURE NOT AVAILABLE FOR GIVEN ALTITUDE)
      CONTINUE
      TYPE 70
      GO TO 100
      PRES=P(I)
      RETURN
      END
      FUNCTION Y(XA)
      DIMENSION WVLNT(100),EFCNCY(100)
      COMMON WVLNT,EFCNCY,NDATA,AT,ALT
      AMOLWT=28.96
      PI=3.1415927
      AK=1.38042E-16
      AC=2.99793E+10
      AH=6.62517E-27
      ANUM=AC*AH
      ADENM=AK*AT*XA
      ARES=ANUM/ADENM
      CALL XYFCN(WVLNT,EFCNCY,NDATA,XA,EFF)
```

```
        AMAV=AMOLWT/6.023E+23
  J=ALT
  IF(J-1000)250,300,300
  AII0=1.
  GO TO 350
  CALL PRESUR(ALT,P)
  ANT=P/(AMAV*G(ALT))
  CHI=0.827286
  AII0=EXP(-(GAM(XA))*((1./(COS(CHI)))*ANT))
  Y=(1./((XA)**4))*(1./(EXP(ARES)-1.))*EFF*AII0
  RETURN
  END
  FUNCTION GAM(XA)
  IF((XA/1.E-08)-20.)10,10,20
  GAM=(1.32E-22)*((XA/1.E-08)**2.789)
  GO TO 50
  IF((XA/1.E-08)-40.)60,70,70
  TYPE 80
  FORMAT(43HK EDGES OF OXYGEN AND NITROGEN IN THIS BAND)
  TYPE 90
  FORMAT(31HPREVENT ANALYSIS OF THIS REGION)
  GAM=(3.9E-23)*((XA/1.E-08)**2.266)
  RETURN
  END
        FUNCTION G(ALT)
  A=7.259E-05*(ALT)**2
  B=-3.086597E-01*(ALT)
  C=9.793244E+02
  G=A+B+C
  RETURN
  END
```

APPENDIX D

FLIGHT PLAN NIKE-APACHE 14.456, 14.457

1.1 PERSONNEL

C. A. Accardo	GCA Corp.	Project Scientist
L. Johnson	GCA Corp.	Engineer
C. Arouchon	GCA Corp.	Engineer
F. Wanko	GCA Corp.	Engineer
Nelson Maynard	NASA	Project Experimenter
G. Sharp	Lockheed	Project Experimenter

1.3.1.4 Payload* Length - 78.38 inches

Payload** Weight - 65 pounds

*Not including S-Band Beacon

**Including S-Band Beacon

1.3.1.6 INSTALLATIONS

1. Solar x-ray detectors 44-60Å, 8-20Å, 2-8Å
2. Epithermal Analyzer Electron detector
3. Electric field and electron probe (two 20-foot antennas extended radially and opposite)
4. Door Release Mechanism, guillotine actuated (Holex 2801)
5. Dual timer, (Raymond Model 1060-5G-180T)
6. Main Batteries (19 Yardney type HR-1 DC cells)
7. Magnetometer, Schonstedt Type Ram 5-C
8. Solar Aspect Sensor, GCA Model XA5-103
9. Pyrotechnic Batteries (14 Yardney HR -1 DC cells)
10. Subcarrier oscillators, eleven (Dorsett MA18K)
11. Mixer Amplifier
12. Transmitter, (Dorsett TR-501A)
13. Antenna, 4-element trunstile, 60° sweep

14. Payload control relays (Potter-Brumfield TL17DA)

15. Barometric switches, 70 KFT (one), 40 KFT (two) (PSI Mod. A37C015, A37C023)

16. Umbilical connector, first motion (Deutsch DM9606-27S)

17. DC-DC converter (Model N9507-106)

18. Commutator, 2 1/2 RPS x 30, BBM (Datametrics Mod. 856)

1.3.1.7 PYROTECHNIC INSTALLATIONS

The door release mechanism consists of a non-explosive Holex guillotine cutter which severs an 8-32 brass screw that retains the door under a light spring pressure of about 2 pounds. Arming of the circuit occurs at 40,000 feet by a barometric switch. Two Raymond timers (for purposes of redundancy), which are G-actuated at launch, provide the time delay to release the door at the required altitude. Door release will occur at approximately 60 km altitude.

In addition to the door release, the pyrotechnic circuit is also used to deploy two 20-foot antenna probes for the Electric Field experiment. The arming barometric switch and Raymond Timer switch complete the circuit to actuate a 20-volt motor which deploys the antennas. Extension time for the antennas is about 60 seconds. They extend through two 1-inch diameter holes in the payload shell.

The circuit diagram for the pyrotechnic installation is shown in Figure D-1.

1.3.2 VEHICLE DRAWINGS

Payload configuration is shown in Figure D-2.

1.4.1 TRANSPONDERS AND BEACONS

An S-band Transponder will be used. This will be supplied by NASA.

1.5.1 TEST PROGRAM OBJECTIVES

The payloads are instrumented to study solar X-ray fluxes in the 44-60Å, 8-20Å, 2-8Å region, and behavior of the ionosphere, during the total solar eclipse of March 1970 at Wallops Island, Virginia. A "background" flight 14.456 will be made the day before the Eclipse, under conditions of the same solar zenith angle as the eclipse. Flight 14.457 will occur during totality. The exact launch time will be determined at a later date.

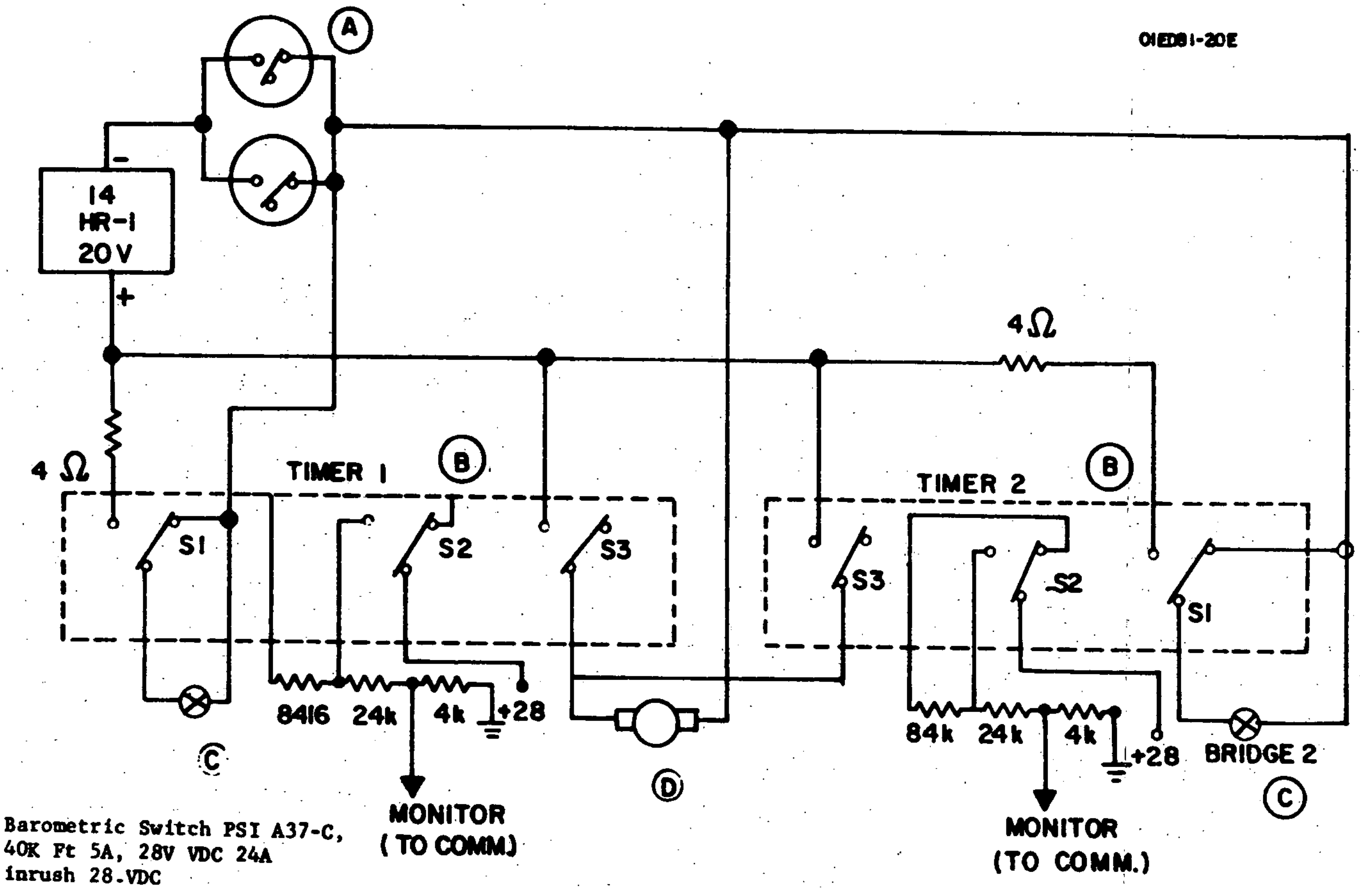

(A) Barometric Switch PSI A37-C, 40K Ft 5A, 28V VDC 24A inrush 28.VDC

(B) Raymond Timer Mod. 1060-5G-180T

(C) Holex Guillotine Cutter 0.66Ω per Bridge

(D) Antenna Motor 400 MA Operating 800 MA Stalled

Figure D-1. Nike-Apache 14.456, 14.457 pyrotechnic circuit.

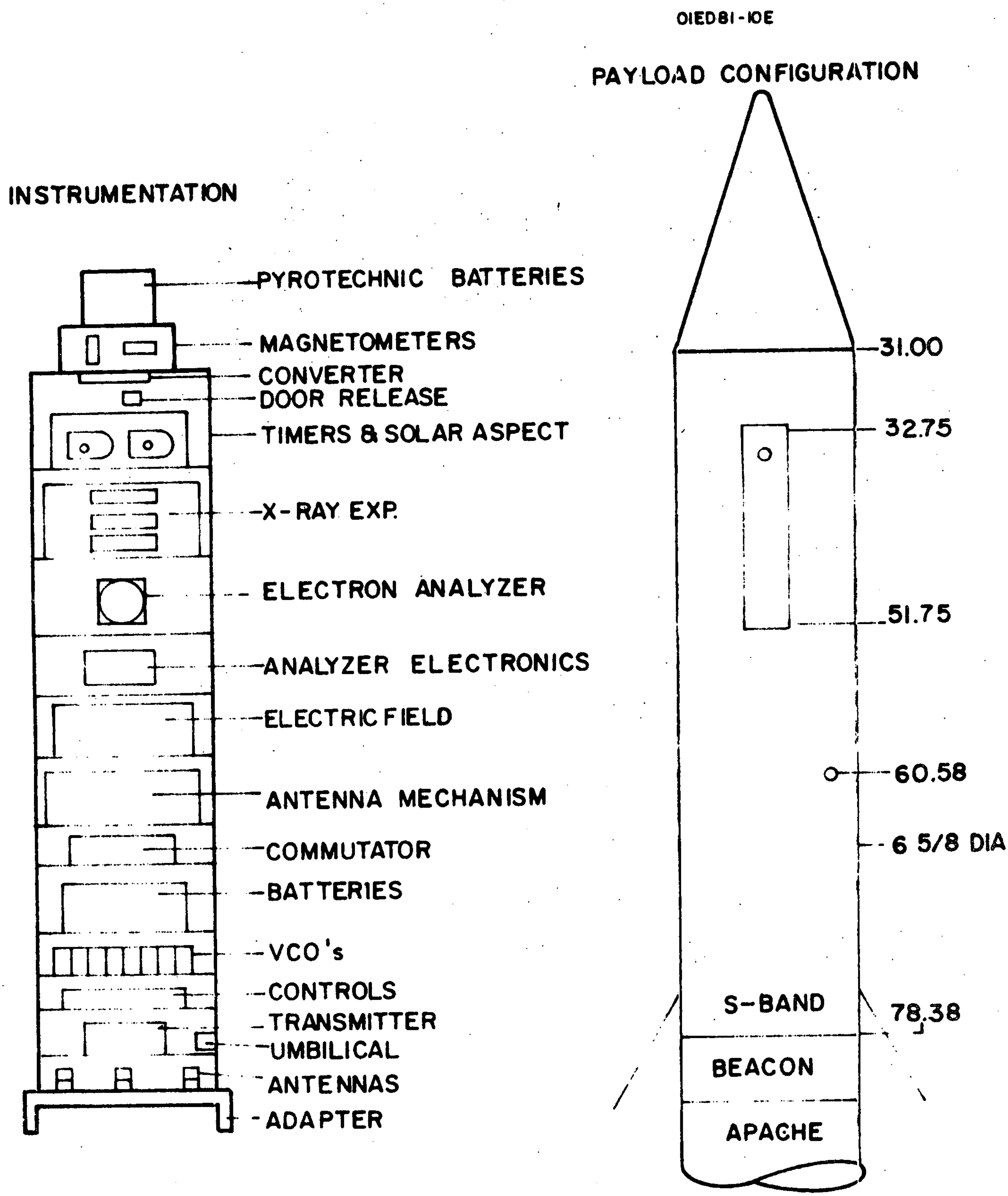

Figure D-2. Nike-Apache 14.456, 14.457 Payload configuration.

1.5.3 PROGRAM OPERATION CONSTRAINTS

The two launches are to be made before and during the total eclipse of 7 March 1970. If weather conditions prohibit launching the day before the eclipse, 14.456 may be launched the day following eclipse. Further, if there is a high degree of magnetic activity the day before the eclipse, 14.456 may be postponed until the day after the eclipse.

1.5.4 LAUNCH PARAMETERS

An effective azimuth of 155° is desired for both flights. The elevation parameter will be between 80 and 83° based upon obtaining the best trajectory within the totality path. This will be determined at a later date.

ADDITIONAL INFORMATION

The payloads will contain a low-level radioactive source (~ 1.0 Microcurie) to stimulate the X-ray detectors. When the door is ejected, at about 60 km, the source which is attached to the door, will be ejected. Note that this also serves to monitor door release.

TELEMETRY CHANNEL ASSIGNMENTS

The transmitter frequency for 14.456 and 14.456 was 219.45 MHz.

Channel assignments are as follows:

Ch. H - Electric Field
Ch. 19 - X-Ray (Mylar) 44-60Å
Ch. 18 - X-Ray (Be) 2-8Å
Ch. 17 - X-Ray (Al) 8-20Å
Ch. 16 - Commutator
Ch. 15 - Electric Field
Ch. 13 - Electric Field
Ch. 12 - Electron Analyzer
Ch. 11 - Solar Aspect
Ch. 10 - Roll Magnetometer
Ch. 9 - Longitudinal Magnetometer

In addition to the above there will be a 21.4 KHz pure sine wave signal which will be transmitted as a sub-carrier. It is required that this signal be recorded on the flight magnetic tape.